21-34-38W

15-189-21007

* * * * *

HYDRAULIC FRACTURE MAPPING

TAYLOR D-1H WELL
HUGOTON FIELD
STEVENS COUNTY, KANSAS

PREPARED FOR

ANADARKO PETROLEUM CORPORATION
2330 NORTH KANSAS AVENUE
LIBERAL, KANSAS 67901

ATTENTION:

MR. BRAD MILLER

PREPARED BY

HUNTER GEOPHYSICS
2344 WALSH AVENUE
BUILDING F
SANTA CLARA, CALIFORNIA 95051
(408)727-9552

* * * * *

522419

Table of Contents

Chris Wright
Mgr. Technical Applications

Hunter Geophysics

2344 Walsh Avenue, Bldg. F
Santa Clara, CA 95051
(408) 727-9552

LIST OF TABLE

LIST OF FIGURES

LIST OF APPENDICES

SUMMARY

On April 24, 1988 Hunter Geophysics used an array of tiltmeters to monitor a hydraulic fracture on the Anadarko Taylor D-1H well. The perforated interval was from 2622 ft. to 2990 ft. A total slurry volume of 2917 BBLS was injected at a rate of approximately 60 BPM. The quality of tiltmeter data was excellent due to the high injection rate and relatively stable background tilt.

Analysis of the tiltmeter data indicates a predominantly vertical fracture system trending N 115 E was created. A horizontal fracture component of slightly less than 10% of the injected volume was also created. A tracer log was run on an adjacent well fracture, the Perrill D-1H, to provide some independent data on the vertical fracture height. The vertical fracture had an azimuth of N 115 E, a dip of 87 deg. (90 deg. is perfectly vertical), with a length of 635 ft., height of 340 ft. (from tracer log data), and a width of 0.89 inches. The horizontal fracture, modeled as forming at the top of the vertical fracture, had a volume of 215 BBLS and was dipping slightly (6 degrees) down-to-the-East.

INTRODUCTION

Hunter Geophysics installed an array of tiltmeter sensors around the Anadarko Taylor D-1H well on April 9, 10, and 11. The instruments had started to settle and were recording continuous tilt data from April 15 until after the stimulation was completed.

This report includes a description of how the data was collected; an overview of the solution for fracture parameters; a discussion of the sensitivity (or uncertainty) of the determination of fracture parameters; and appendices covering the basics of Tiltmeter Fracture Mapping Technology, a review of the geophysical inversion process (fracture solution techniques), and Hunter's most recent technical publication.

DATA COLLECTION

Tiltmeter installation was completed on April 11, and by April 15 the instruments had settled enough to collect meaningful background data. All tiltmeters had cables running to a central data acquisition system where the output was converted to digital format and stored on floppy disks. The output from each tiltmeter was continuously sampled at one minute intervals.

The background noise, particularly on the high frequency end, was sufficiently small to allow the tilt signal due to the stimulation to appear within a few minutes of the start of the injection. Figures (1), (2), and (3) show raw tilt data from six channels. The dashed red lines indicate the break-down and shut-in times of the stimulation. A separate analysis of each channel is performed to determine the stimulation induced tilt on each channel (details of this can be found in Appendices I and III). Table (1) shows the location and stimulation induced tilt for all channels of all instruments. This data is the required input to the theoretical models to solve for fracture source parameters.

FRACTURE SOLUTION

After the analysis is complete for the stimulation induced tilt on all channels (the observed tilt field), the geophysical inverse problem can be solved for the fracture source parameters. Some details of this process are contained in the Appendices.

The models used to solve for source parameters are functions of all source variables (fracture azimuth, dip, depth, length, height, width, and offset coordinates of the fracture center from the wellbore). Solution for fracture azimuth and dip (and whether fracture structure is complex) is independent of all other parameters. There exists, however, some mathematical coupling between the remaining source parameters that leads to greater uncertainty in

their precise determination (the actual degree of uncertainty is dependent upon the specifics of the job). If independent sources of information exist regarding any of the fracture parameters, this information can be used to lower the uncertainty in the determination of the remaining parameters. Tracer log information regarding fracture height was obtained on the nearby Perrill D-1H well and was used as a height constraint on the fracture solution for the Taylor D-1H well. This final fracture mapping report will utilize the height data obtained from the tracer log (fracture height of 340 ft. and depth to center of 2826 ft.). Earlier Field Reports were submitted to Anadarko with height constraints from formation data (April 24, 1988), and with no constraint on height growth (May 17, 1988).

Figure (4) shows the vector overlay of observed and theoretical tilt vectors for the best-fit fracture solution for the Taylor D-1H well. The fracture system was complex, with a small (7% of injected slurry volume) horizontal cap on the dominant vertical fracture. The vertical fracture had an azimuth of N 115 E and a dip of 87 degrees (90 deg. dip is purely vertical). The 3 degree rotation away from the vertical is down-to-the-NorthEast. The vertical fracture was 635 feet long (uncertainty of this measurement is covered in the next section), 340 feet high (from tracer log), and 0.89 inches wide. The horizontal fracture was dipping 6.0 degrees down-to-the-East and had a volume of 215 BBLS and an aperture (width) of 0.56 inches. The fracture source parameters are all listed at the bottom of Figure (4). Note that the solution error for this fracture system is 9.8% , this is an exceptional fit and will be compared to solution errors for other fracture source parameters in the following section.

A separate analysis was done of the data constraining the solution to be a single planar fracture. Figure (5) shows the overlay of observed and theoretical tilt vectors for the best-fit simple (single planar structure) to the observed tilt data. The solution error is 26.1%, which is 166% higher than the best-fit fracture system solution. This discrepancy, while very large, is not the sole factor used to justify the existence of a complex fracture. An examination of Figure (5) shows that sites perpendicular to the strike of the fracture (sites 2 and 10) have theoretical and observed vectors pointing in the same direction, towards the strike of the fracture. As you move away from these sites the observed vectors are rotated away from the strike of the fracture. This is the effect a horizontal component has on the tilt field of a predominantly vertical fracture system.

To investigate the uncertainty with respect to fracture parameters, all parameters except one are held constant at their best-fit values and the remaining parameter is allowed to vary. The degree of uncertainty is reflected in the change in value of the solution error as the parameter of interest is varied. Figure (6) shows an overlay of observed and theoretical tilt vectors for the same fracture system with the azimuth rotated 20 degrees to N 95 E. Clearly one can see the fit is not nearly as good, in fact the solution error has increased by 260% .

Figures (7), (8), (9), and (10) show plots of solution error versus dip of the vertical fracture, azimuth of the vertical fracture, volume of the horizontal fracture, and length of the vertical fracture, respectively. One possible uncertainty criterion is to deem (choose as) significant a certain percentage increase in the value of the solution error from the minimum solution error. For Figures (7) through (10) the best-fit value is indicated at the minimum of the solution error, and bounding lines are indicated where the solution error is 30% greater than the minimum solution error. Of course the choice of 30% is arbitrary, one may desire to choose 10% or 100% . Using the 30% criterion, the bounds on each of the parameter is; dip: 85 - 90 deg.; azimuth: N 108 E - N 121 E; horizontal volume: 125 BBLS - 320 BBLS; vertical fracture length: 550 ft. - 740 ft.

ANADARKO Taylor D1H

Site #	Instr. #	Tiltmeter locations (ft.) E-W (X)	N-S (Y)	Channel #	Observed Tilt Values (nanoradians) X-chan	Y-chan
1	561	0.0	1000.0	1, 2	-53.8	-58.6
2	536	382.7	923.9	3, 4	-16.4	-82.9
3	535	707.1	707.1	5, 6	-15.5	-109.6
4	509	923.9	382.7	7, 8	-16.0	-107.7
5	544	991.2	44.1	9, 10	-0.6	-44.1
6	528	923.9	-382.7	11, 12	27.7	35.2
7	525	707.1	-707.1	13, 14	35.7	68.8
8	541	382.7	-923.9	15, 16	36.5	100.4
9	507	0.0	-1000.0	17, 18	69.6	80.5
10	526	-382.7	-923.9	19, 20	7.0	78.9
11	931	-707.1	-707.1	21, 22	-13.2	151.4
12	927	-923.9	-382.7	23, 24	6.0	160.7
13	940	-1000.0	0.0	25, 26	20.8	51.2
14	937	-923.9	382.7	27, 28	8.3	5.6
15	928	-707.1	707.1	29, 30	-35.4	-34.5
16	919	-382.7	923.9	31, 32	-38.7	-52.1

TABLE 1. Instrument locations and observed tilt values.

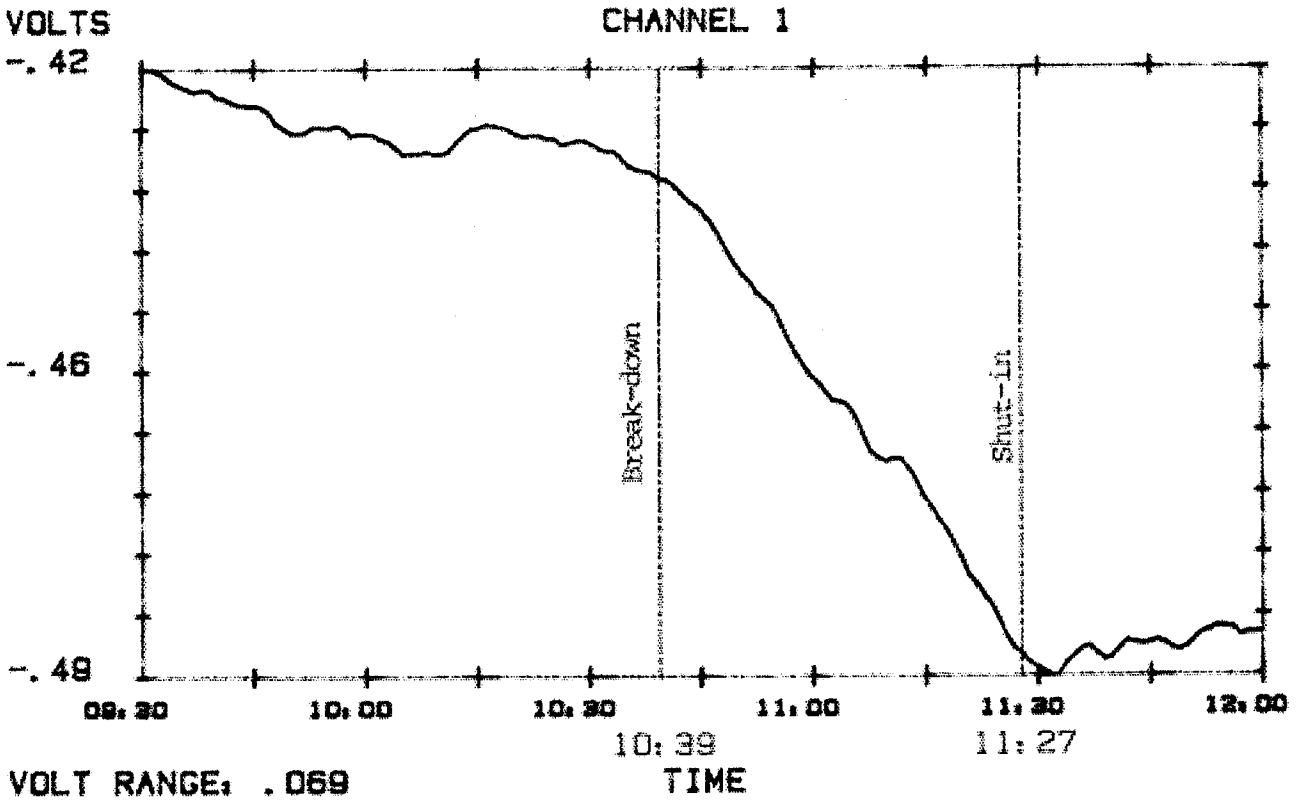

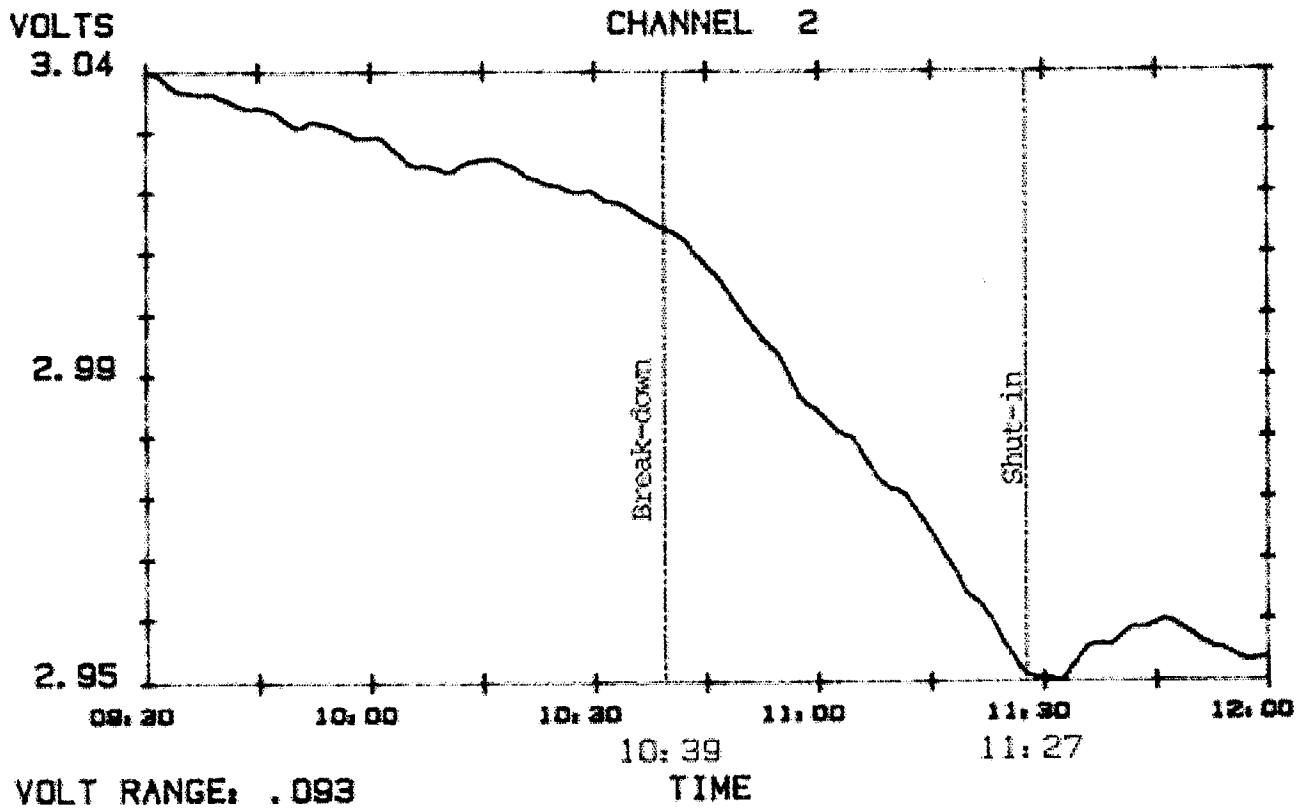

START 04: 24: 09: 30: 00
STOP 04: 24: 12: 00: 00
EVENT (HR: MN) _____

HUNTER GEOPHYSICS 1988

Figure 1. Raw Tilt Data From Site #1.

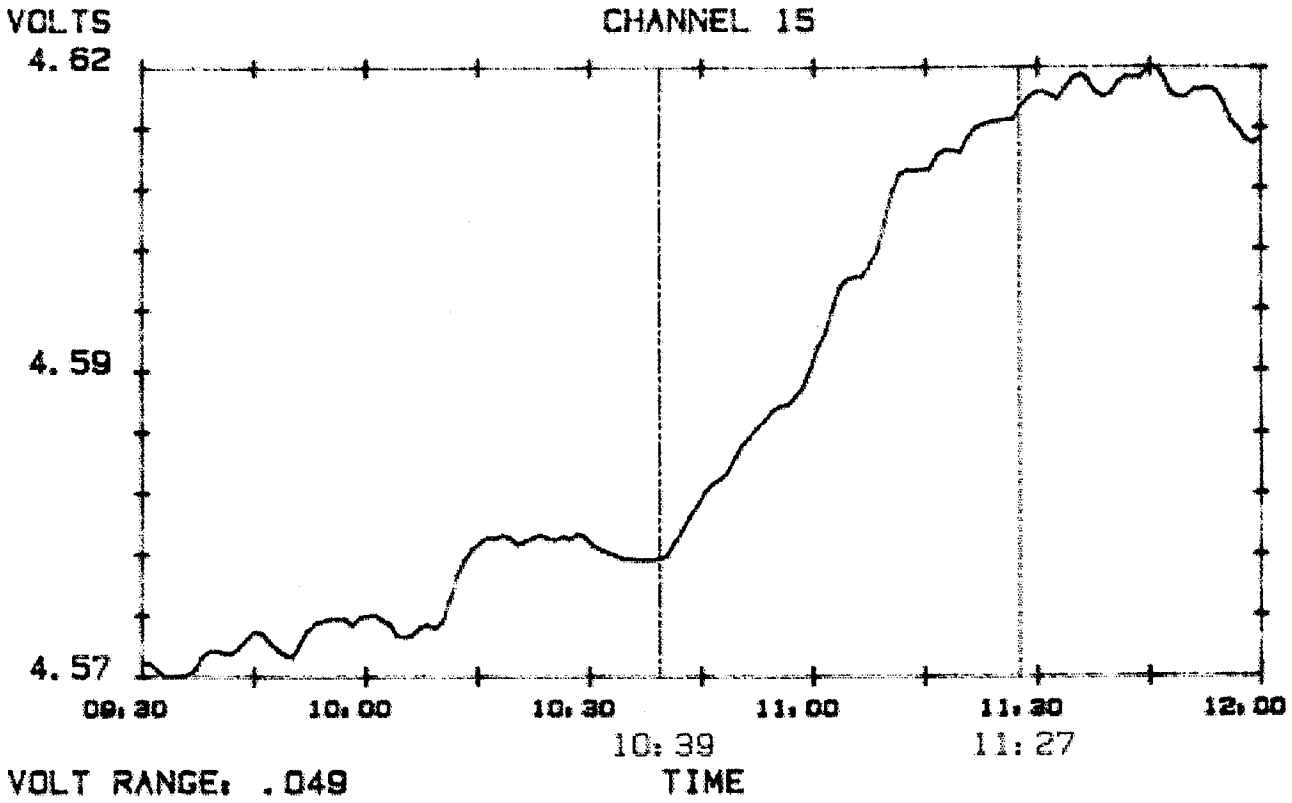

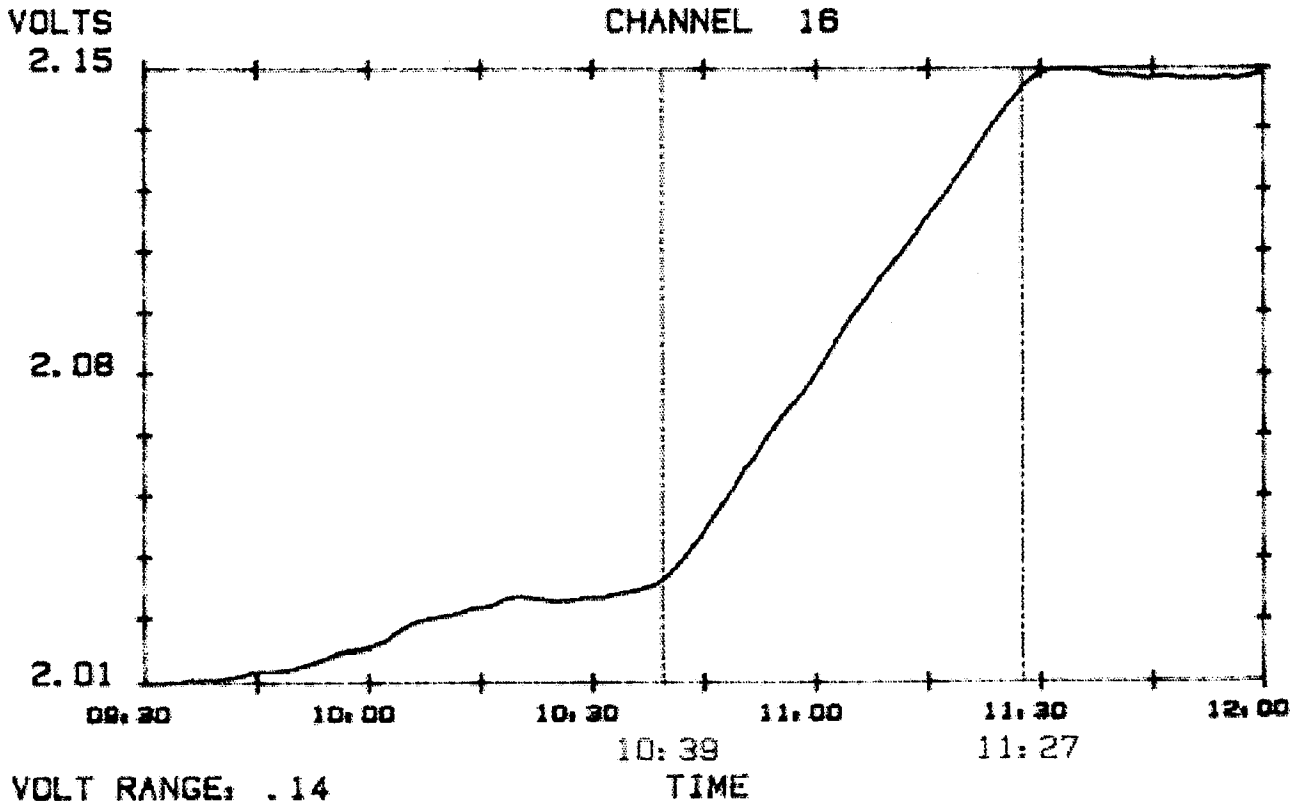

START 04:24:09:30:00
STOP 04:24:12:00:00
EVENT (HR:MN) _____

HUNTER GEOPHYSICS 1988

Figure 2. Raw Tilt Data From Site #8.

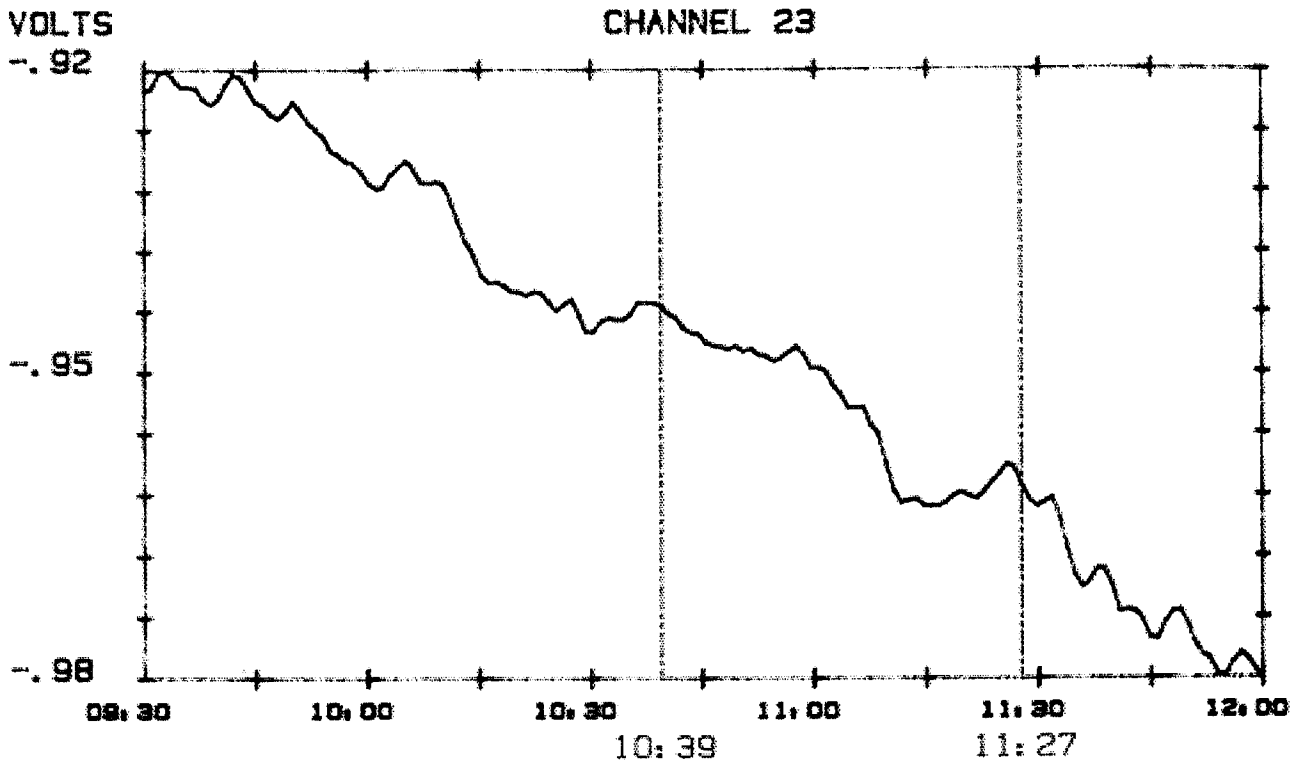

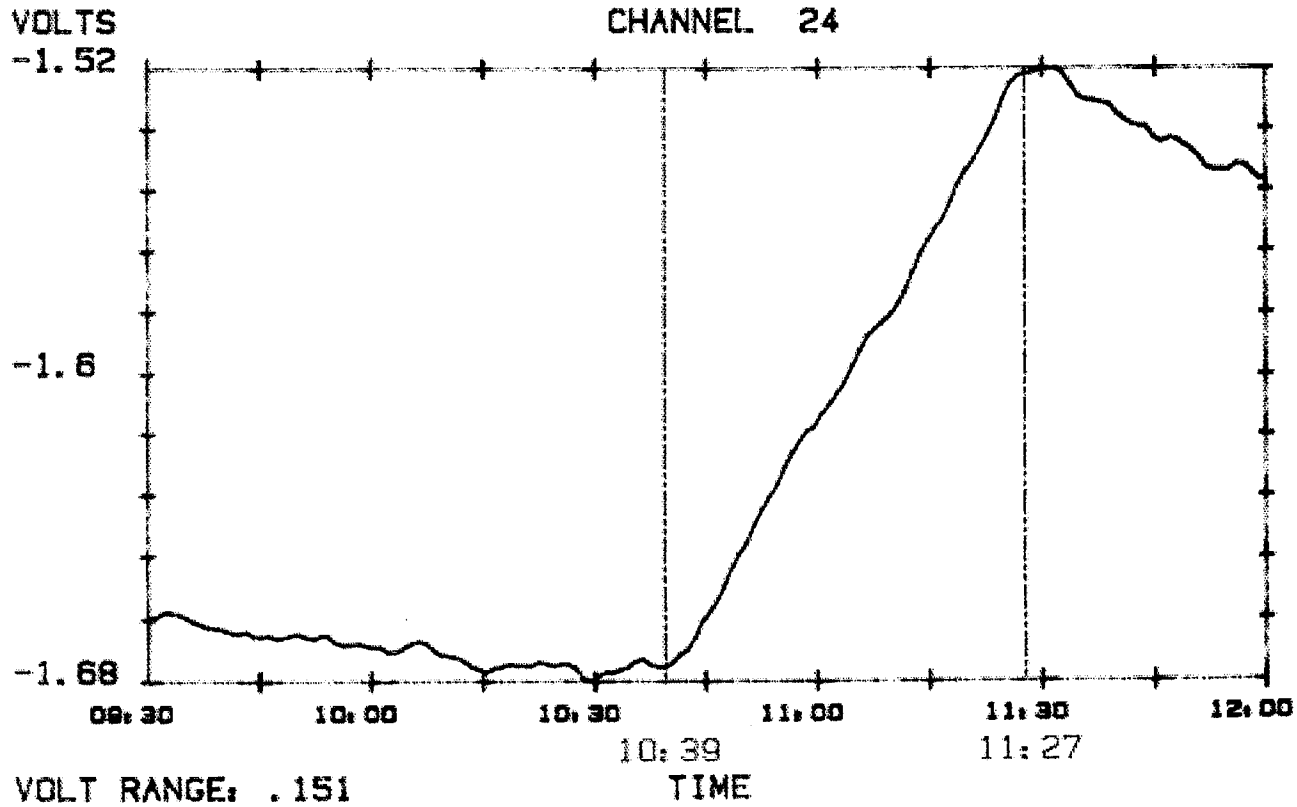

START 04:24:09:30:00
STOP 04:24:12:00:00
EVENT (HR:MN) _____

HUNTER GEOPHYSICS 1988

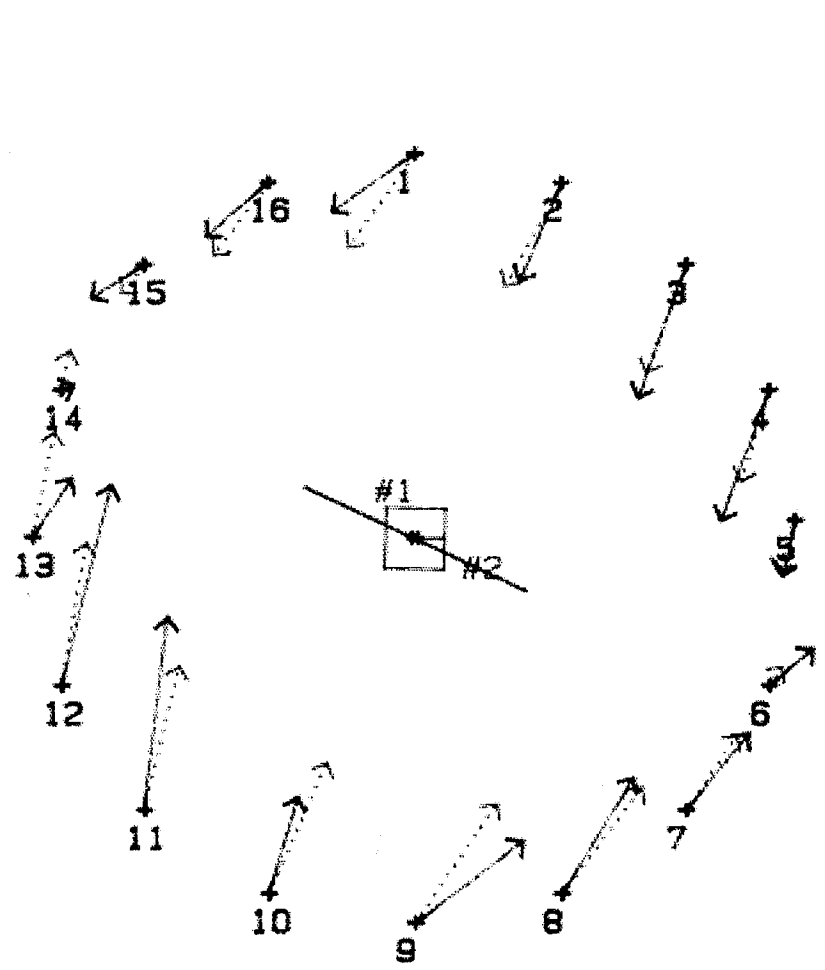

WELL: ANADARKO Taylor D1H
DATE: 4/24/88

.15 uRAD
REAL
THEO

FRAC #	AZ	DIP	DEPTH (FT)	L*H*W (CU FT)
1	115	87	2826	635 * 340 * .074
2	2	6	2660	160 * 160 * .047

Theoretical and observed vector overlay on best-fit complex fracture system with constrained height on vertical fracture. Solution error = 9.8%

HUNTER GEOPHYSICS 1987

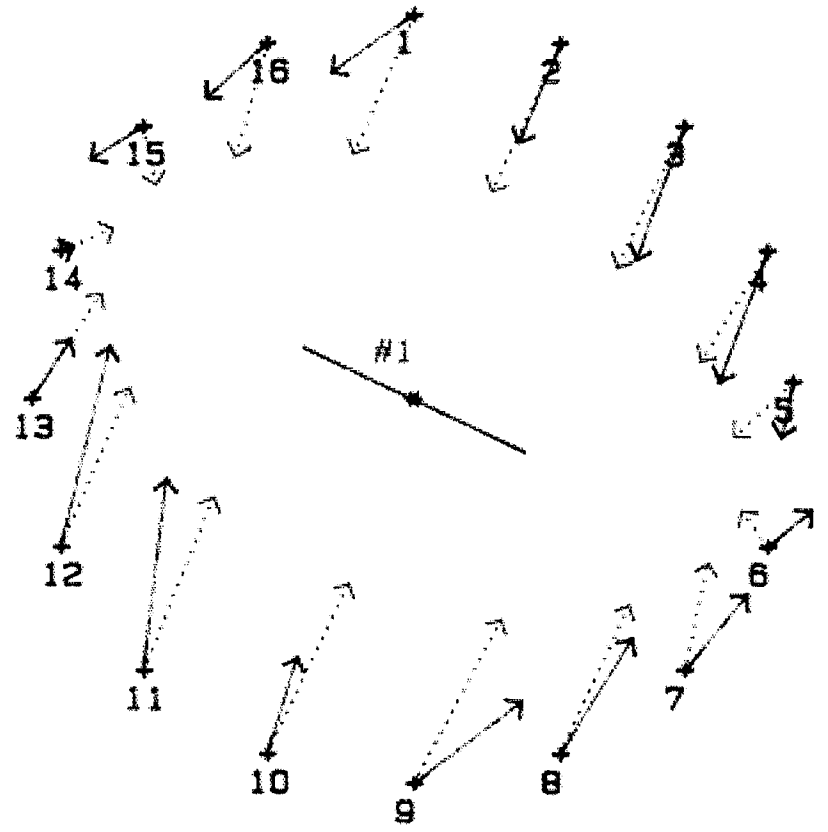

WELL: ANADARKO Taylor D1H
DATE: 4/24/88

.15 uRAD
REAL
THEO

FRAC #	AZ	DIP	DEPTH (FT)	L*H*W (CU FT)
1	115	87	2826	635 * 340 * .074

Theoretical and observed vector overlay on best-fit simple (vertical) fracture system with constrained fracture height. Solution error = 26.1%

HUNTER GEOPHYSICS 1987

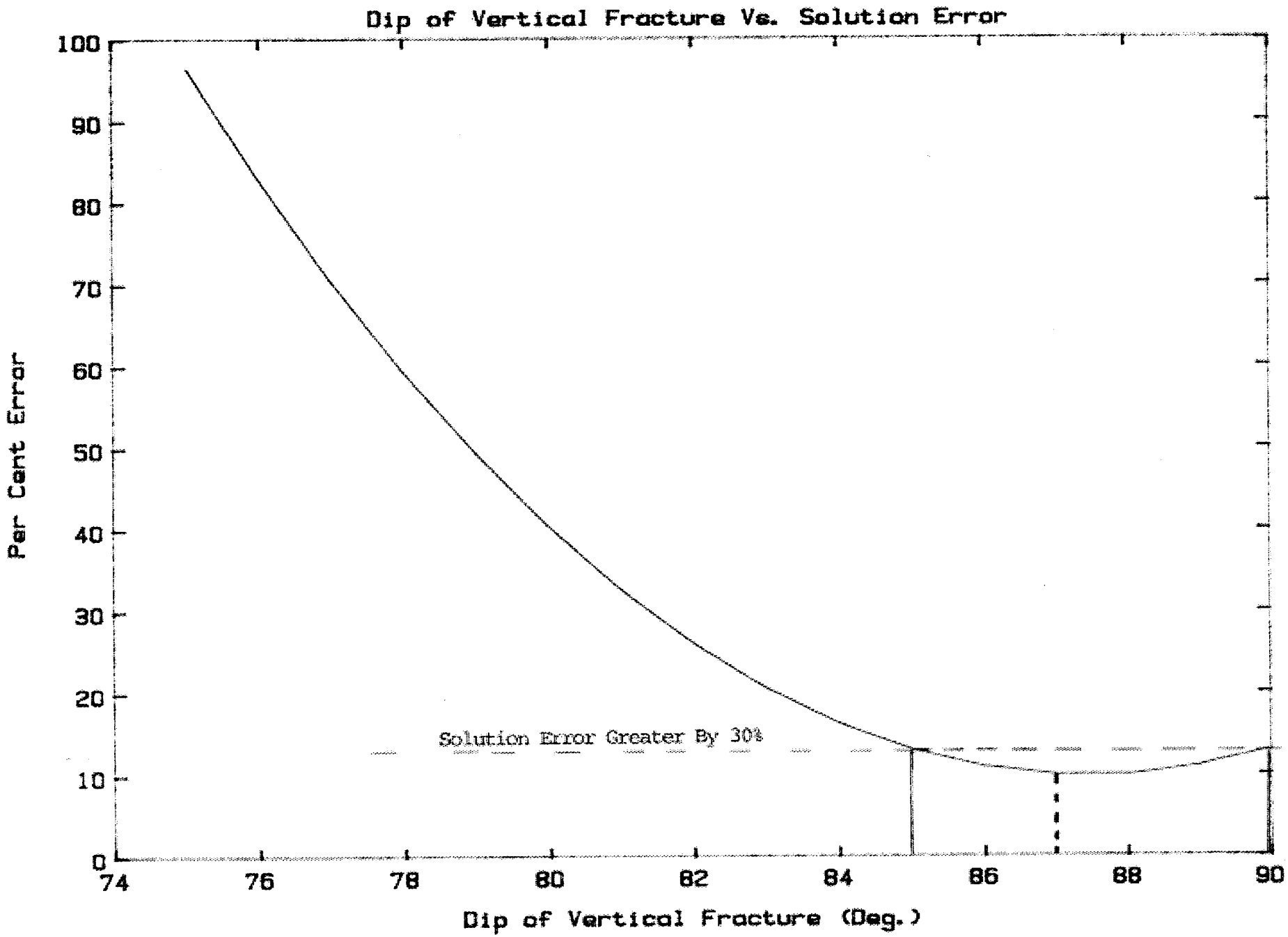
Dip of Vertical Fracture Vs. Solution Error
Per Cent Error
100
90
80
70
60
50
40
30
20
10
0
Solution Error Greater By 30%
74
76
78
80
82
84
86
88
90
Dip of Vertical Fracture (Deg.)

Figure 7.

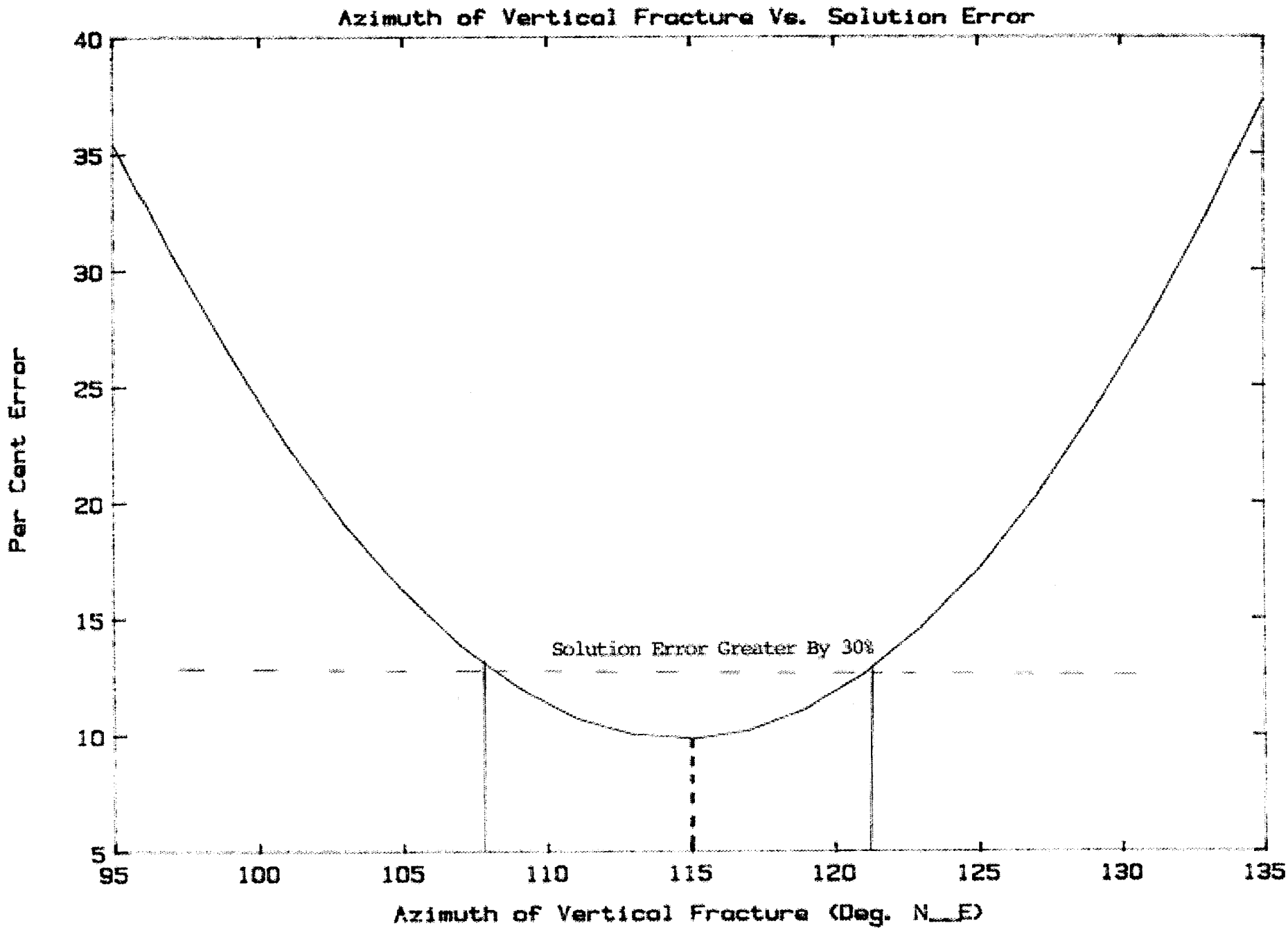
Azimuth of Vertical Fracture Vs. Solution Error
Per Cent Error
40
35
30
25
20
15
10
5
95
100
105
110
115
120
125
130
135
Solution Error Greater By 30%
Azimuth of Vertical Fracture (Deg. N__E)

Figure 8.

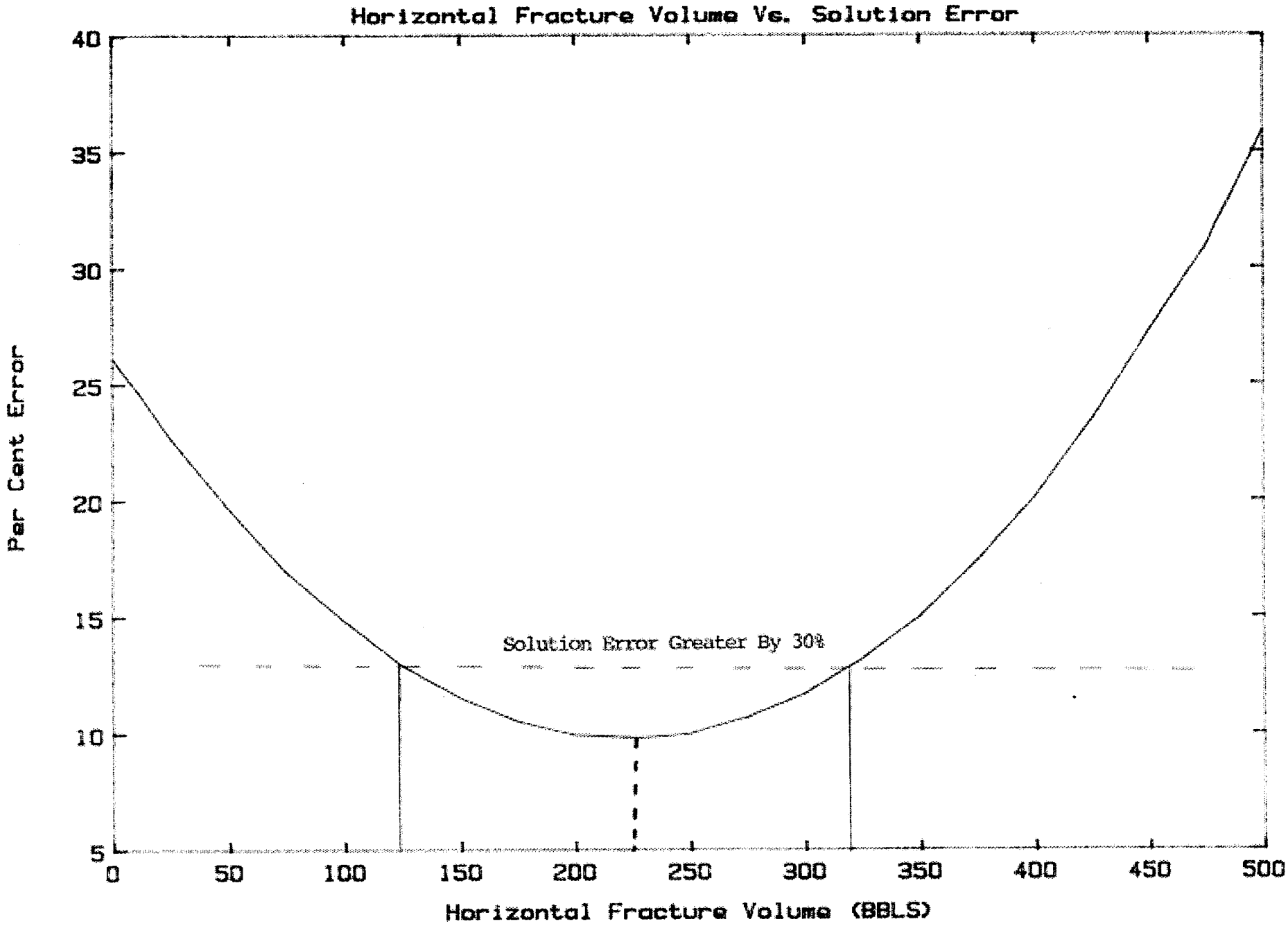
Horizontal Fracture Volume Vs. Solution Error
Per Cent Error
40
35
30
25
20
15
10
5
Solution Error Greater By 30%
0
50
100
150
200
250
300
350
400
450
500
Horizontal Fracture Volume (BBLS)

Figure 9.

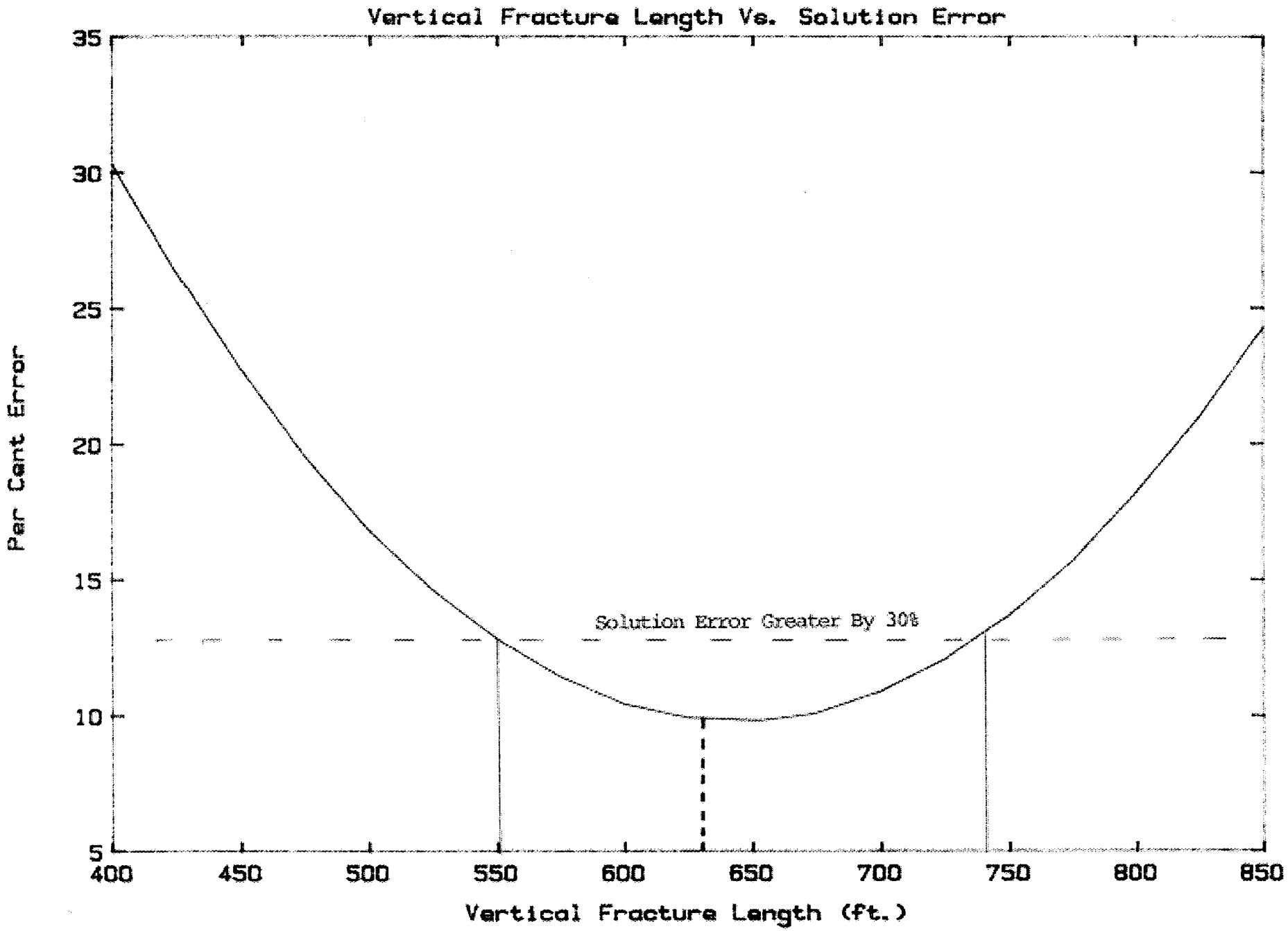
Vertical Fracture Length Vs. Solution Error
Per Cent Error
35
30
25
20
15
10
5
Solution Error Greater By 30%
400
450
500
550
600
650
700
750
800
850
Vertical Fracture Length (ft.)

Figure 10.

APPENDIX A

A Brief Review of Mapping Hydraulic Fractures with Tiltmeter Technology

FRACTURE SOLUTION

After tilt data is collected and analyzed to determine the tilt signals due to the hydraulic fracture stimulation, an inverse problem is solved to determine the nature of the source that produced the observed tilt field. Various models exist that predict surface deformations due to subsurface disturbances. Currently a dislocation model is used to calculate the theoretical surface deformation (and therefore tilt field) due to hydraulic fractures with arbitrary dimensions or orientation. Figure 6 shows the surface deformation resulting from a horizontal fracture and a vertical fracture. Note the fundamental difference in both the shape and amplitude of the induced deformations.

Figure 7 shows a cross section of the surface deformation for a vertical fracture, with the cross section being perpendicular to the "strike" or azimuth of the hydraulic fracture. For instruments located away from the fracture by a distance equal to roughly 40% of the depth, the tilt is maximum, and is down toward the fracture. Thus a theoretical tilt vector array for a North-South vertical fracture would appear as seen in Figure 7b. Figure 8 shows tilt vector patterns for both a vertical and a horizontal fracture.

Graphically, the solution to source parameters is found when there is a best fit match between observed and theoretical tilt vectors. The solution for source parameters that best fit the observed tilt field is obtained by a numerical minimization technique. An error functional (error criterion) is defined as the sum of the squares of magnitude of vector differences between observed and theoretical tilt vectors at each instrument location. The error functional, being a function of source parameters, is minimized by iterating over the possible range of source parameters. Ranges of possible source parameters can be constrained if specific information is known about the formation being stimulated or if conclusions can be drawn from other monitoring data (pressure analysis, temperature logs, radioactive tracers, etc.). Source parameters that give a minimum value of the error functional are considered best estimates of the actual fracture parameters.

Once the "best-fit" fracture parameters are found a sensitivity analysis can be performed for certain parameters of interest. This is done by holding all other source parameters constant, and varying one parameter away from the best-fit value and observing the value of the error functional. A high sensitivity, and therefore a low uncertainty, for a given parameter would see the error functional greatly increase with only small movements away from the best-fit value. Fracture solution has the highest sensitivity to fracture dip, followed by fracture azimuth, then depth, dimensions, and location of the fracture source.

Your fracture report contains sensitivity plots for fracture dip, azimuth, vertical fracture length, and horizontal fracture volume.

COMPLEX FRACTURES

In some cases the error functional minimization yields a solution that still has a significant error between observed and theoretical tilt vectors. This can occur due to a very low signal-to-noise ratio, where there is great uncertainty in measuring the surface tilt field. In cases where expected tilt-signal magnitudes are very small or environmental noise is extremely high across the whole array, the solution for fracture source parameters may not be possible. In the case of poor fit due to poor signal-to-noise ratios, tilt vectors will represent, by definition, noise. There is, however, another possible scenario:

Array processing techniques can determine whether a group of error vectors (the vector difference between observed and theoretical tilt vectors) across an array are in some fashion coherent, spatially low frequency, or are spatially random (measurement noise). Details of this are omitted due to complexity of the argument. The result is that in some cases high residual errors at the end of a best-fit minimization are not due to poor data quality but instead are due to insufficient model accuracy. In these cases, the remaining error vectors are not random, but display a regular pattern across the array. Experience has shown that if the single fracture model is expanded to include more complex fracture structures, then a quality of fit more commensurate with observed signal-to-noise ratio is possible. It has been found that fracture growth can change in orientation during a stimulation, or even grow in two planes simultaneously.

SCHEMATIC OF TILT SENSOR

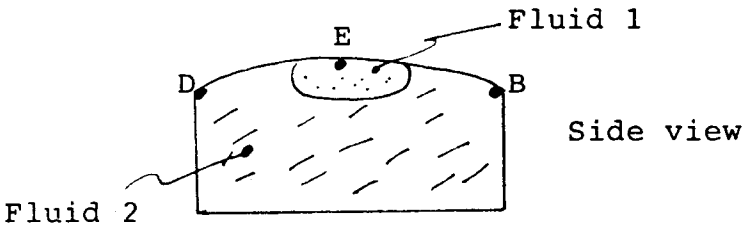

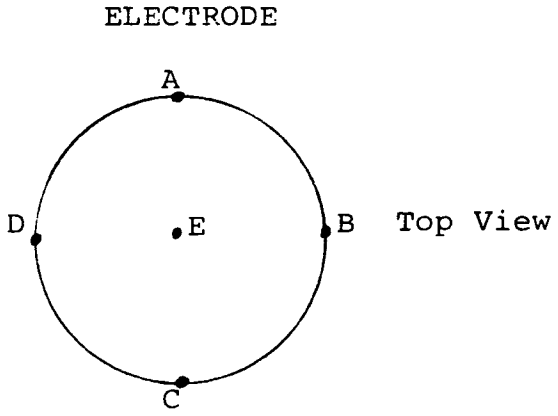

Schematic of Two-Axis Tilt Sensor
Utilized in Hunter Geophysics Tiltmeters.

Figure 1

Typical Tiltmeter Installation

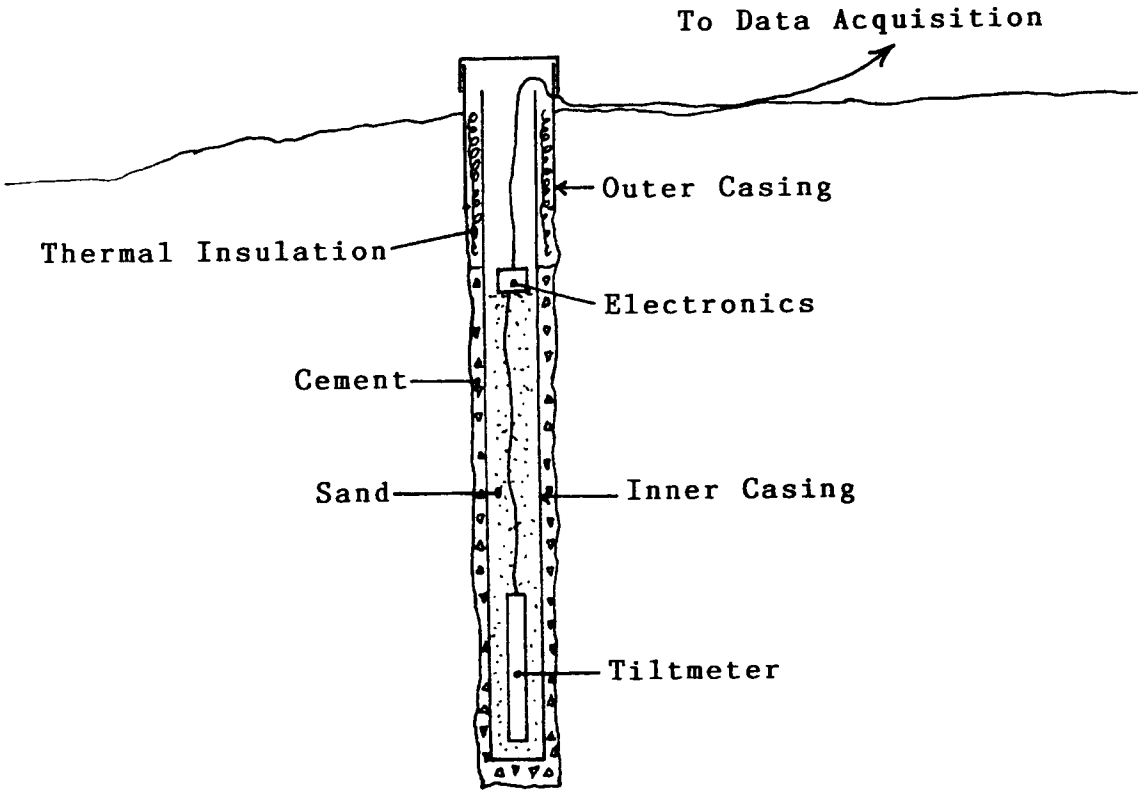

Figure 2

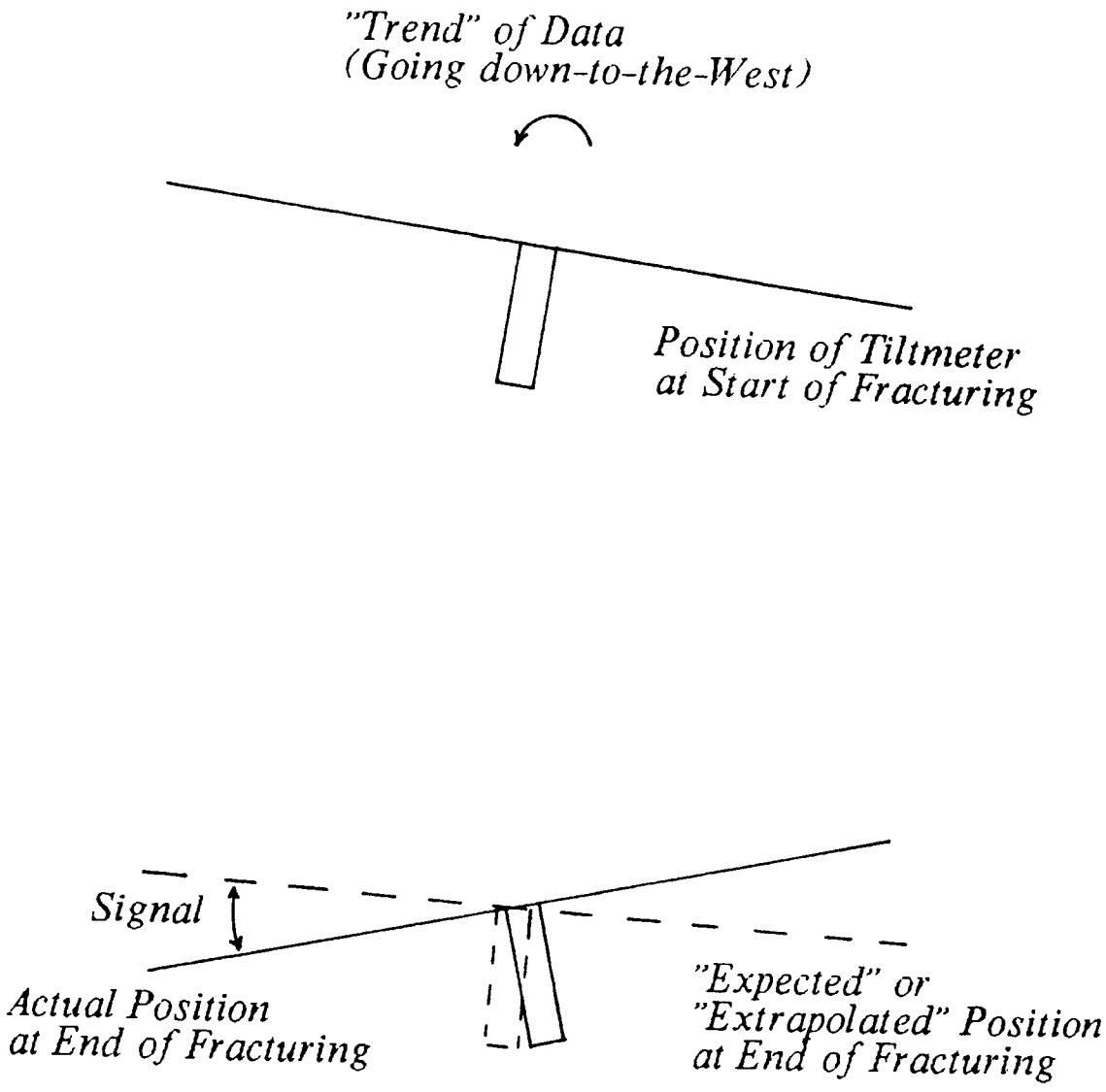
"Trend" of Data
(Going down-to-the-West)
Position of Tiltmeter
at Start of Fracturing
Signal
Actual Position
at End of Fracturing
"Expected" or
"Extrapolated" Position
at End of Fracturing

Figure 3

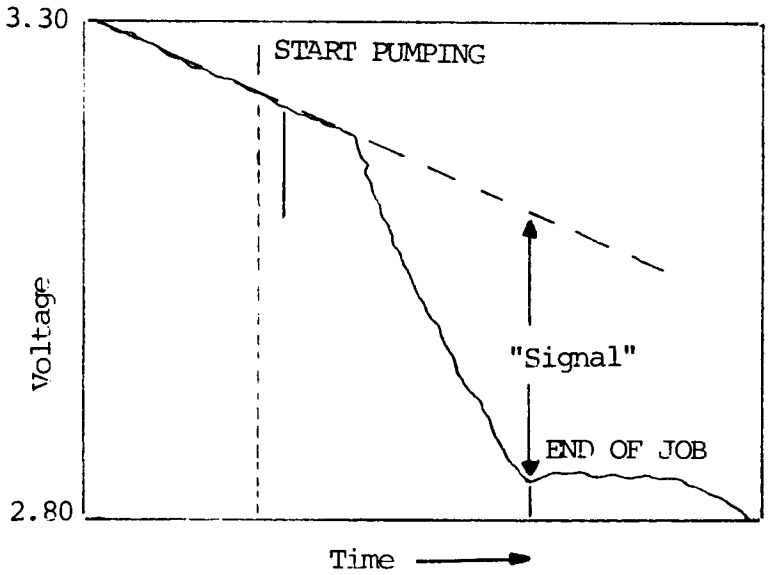

Raw "East-West" Tilt Data From a Tiltmeter Located Approximately 100 feet North-West of a Well Which is Approximately 2000 feet Deep.

Figure 4 - Typical Tilt Signal and Example of Picking Hydraulic Related Tilt.

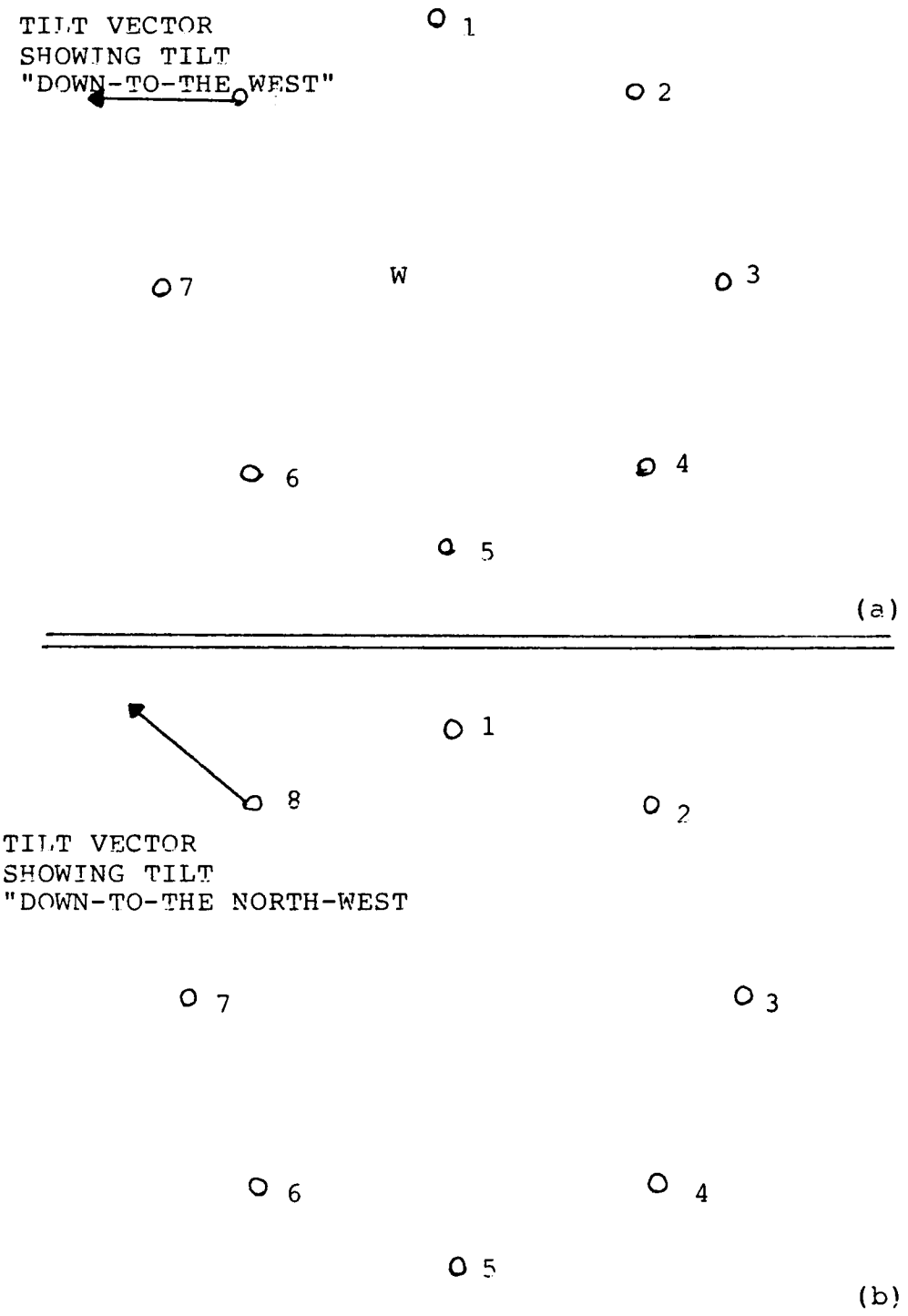

Figure 5 - TYPICAL TILT VECTOR MAP

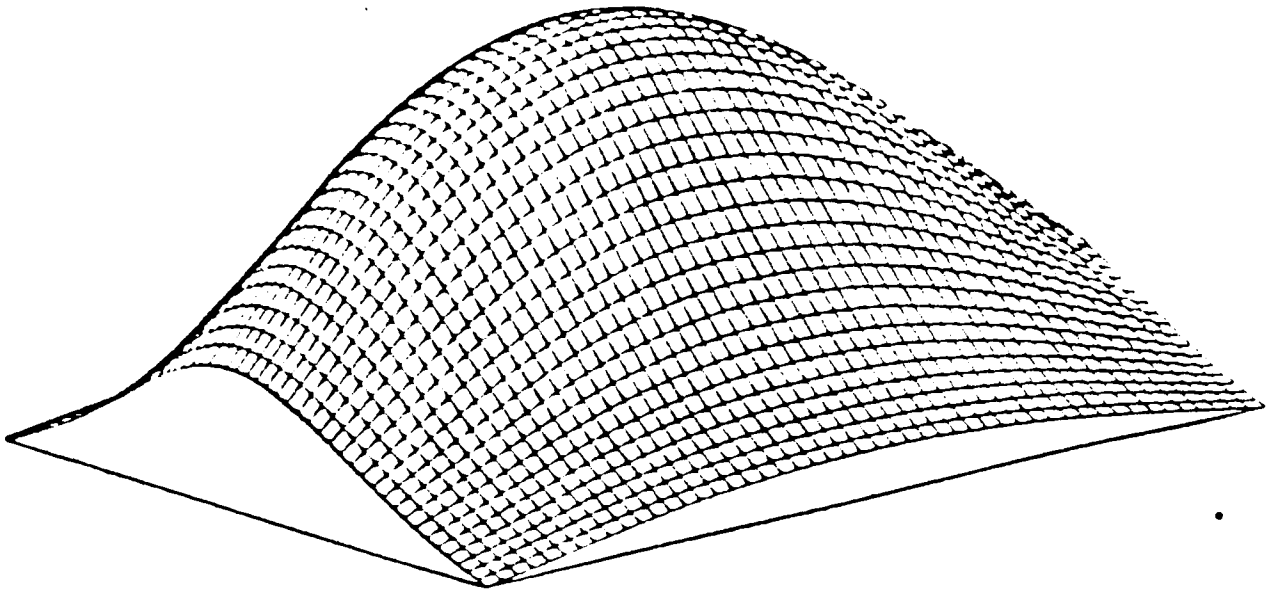

HORIZONTAL FRACTURE

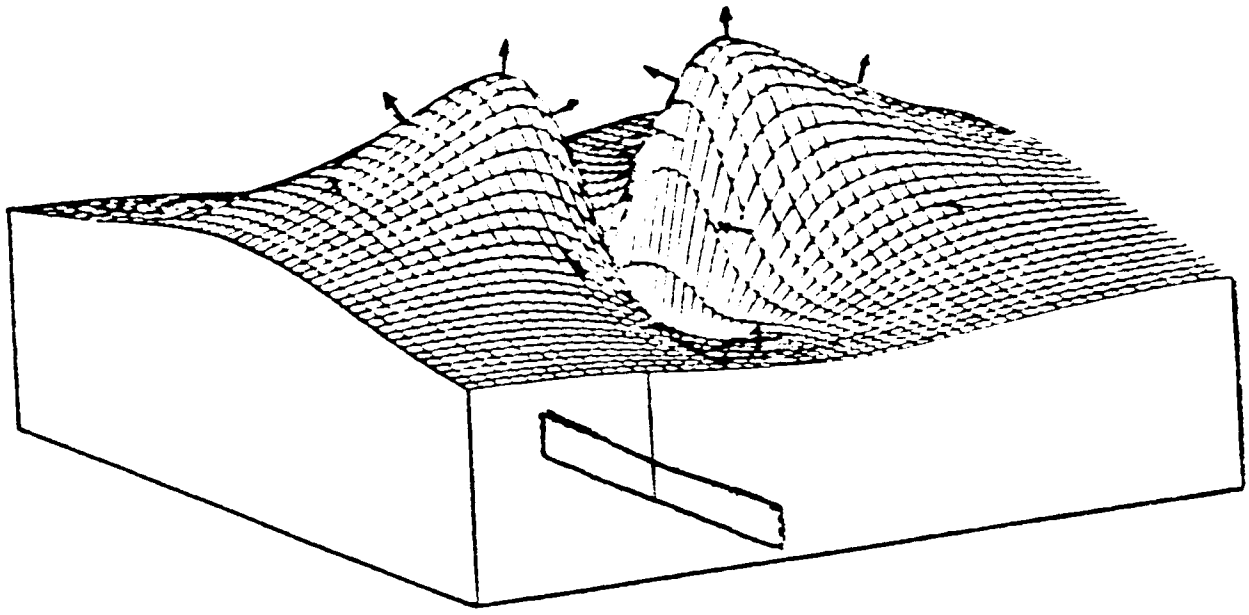

VERTICAL FRACTURE

HYDRAULIC FRACTURE INDUCED
SURFACE DEFORMATION

Figure 6

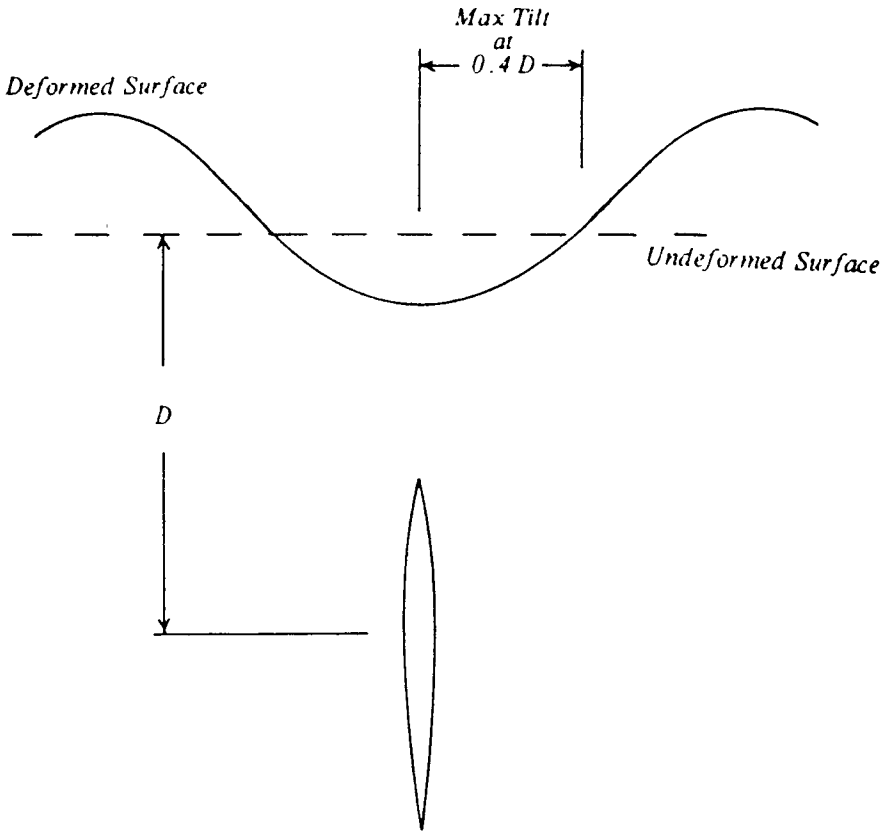

Surface deformation (a) and Tilt vectors for a vertical fracture (b).

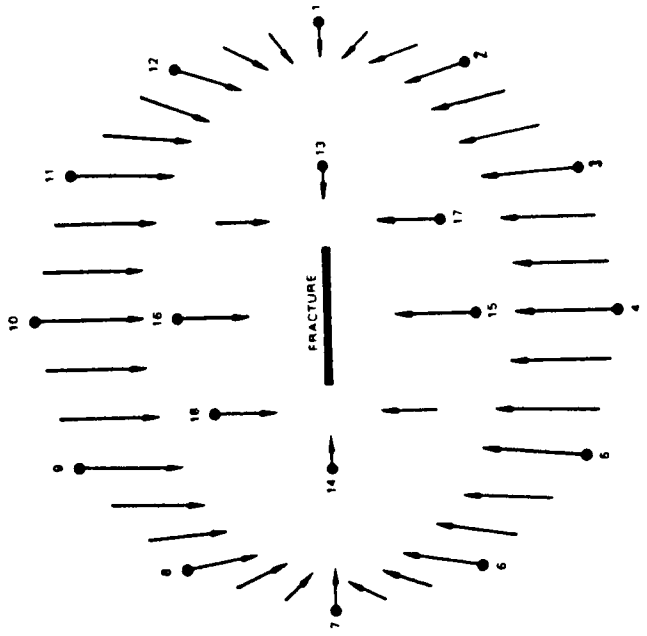

Figure 7

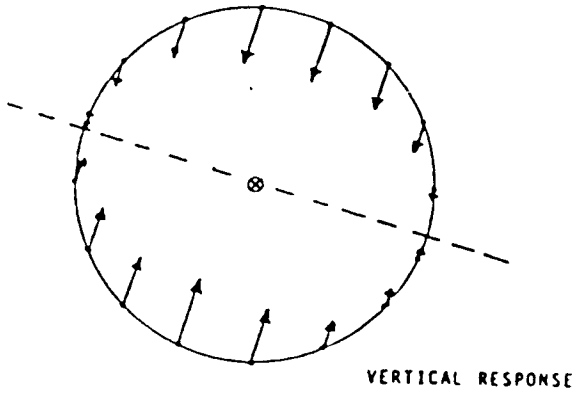

Tilt Vector "patterns"
for horizontal and
vertical fractures.

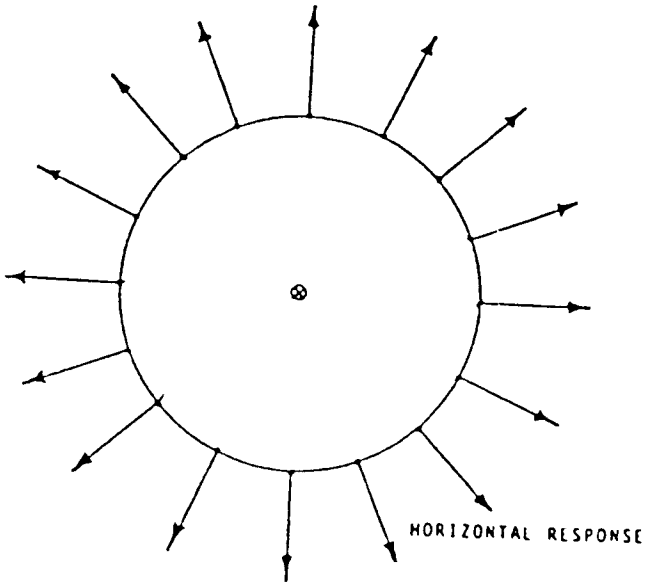

Figure 8

The determination of the physical properties of the earth's interior from data obtained at the earth's surface (such as gravity, free oscillation, seismic, etc.) is known as the "inverse problem" in solid earth geophysics. The techniques employed to solve the inverse problem include: 1) Monte Carlo methods, 2) Hedgehog methods, and 3) General linear inverse methods (see for example Kanasewich,(1973) and Pilant,(1979) for a review of these methods).

Hunter Geophysics employs a non-linear inverse routine (generalization of method 3) above) that inverts observed tilt data to obtain best-fit (least squares) estimates of fracture parameters. The inversion scheme is akin to deconvolution methods used to optimize digital filters (Oppenheim and Schafer, 1975). Fracture parameters are the set of coefficients or constants that occur in the theoretical expressions for surface tilts induced by a dipping hydraulic fracture (solution to the forward problem, Davis,(1983)). Fracture parameters include: fracture azimuth (0-north, 90-east, 180-south, -98-west, -180-south; fracture dip (0-horizontal, 90-vertical); fracture length, l , is measured along azimuth; fracture height, h , is measured down-dip; fracture width, w , is measured normal to the fracture plane; fracture depth, d , is measured positive downwards from the surface, and is normally taken as the center of the perforation interval; fracture center coordinates, wc1, wc2, are measured relative to the well-head, x-positive east and y-positive north; Poisson's ratio, nu, based upon thermodynamic considerations for isotropic media ranges from $-1 > nu > 1/2$, although experimental values for $nu < 0$ are lacking.

Error is introduced into the solution of the inverse problem from essentially two sources: 1) Poor tiltmeter data quality as resulting from low signal to noise ratios, (S/N), and 2) inaccurate choice of models for the hydrofracture process.

The S/N is improved if the tilt sensor is effectively coupled to the earth at depths which are sufficiently shielded from thermoelastic strains (the optimum depth, on the order of 15 feet, is a function of the coefficient of thermal expansion of the soil). Further enhancement of S/N is possible by placing the tilt sensors at surface locations that theoretically yield the maximal tilt response. Maximum tilts for horizontal and vertical fractures in the opening mode occur at a radial distance from the well-head equal to about 40 percent of the depth to the center of the fracture . Hunter can further enhance S/N with the use of an extensive arsenal of proprietary signal processing software which includes: detrending, stacking, time and frequency domain filtering, time series extrapolation based on the Burg algorithm, etc.

At present Hunter employs a dislocation model as the solution to the forward problem. The hydraulic frcture is modelled as a rectangular, uniformly thick dislocation which resides in an homogeneous, isotropic elastic half-space. Real-world departures from these idealizations, which can include material inhomogeneity, anisotropy, inelasticity, etc., will introduce error in the estimates of the fracture parameters even if the tilt data is of excellent quality.

A number of recent attempts to emulate poro-elastic behavior (leakoff), exists in the petroleum engineering literature (for 2-d models based on complex variable methods see Rice and Cleary (1976), pressure decline analysis Nolte (1979), Smith (1981), and Lagrangian methods, Biot et al (1986), while Cleary et al (1983) alone have developed a 3-d model based on finite element and surface integral techniques). Material anisotropy and fracture surface loading conditions also influence the form and magnitude of surface tilts yet only 2-d models to date have addressed these problems (see Pollard and Holzhausen (1979), and Gazonas (1985).

LEAST-SQUARES FIT TO THEORETICAL TILT DATA

The theoretical expression which governs surface tilts induced by a dipping hydrofracture can be expressed as:

$$\text{Tilt} = \frac{\partial v}{\partial x} = f\left(a_1, a_2, a_3 \ldots, a_i\right) \qquad (1)$$

where the a_i are the fracture parameters. A goodness-of-fit measure commonly used in least-squares analyses is the chi-square statistic, defined by:

$$\chi^2 = \sum_{i=1}^{n} \left\{ \frac{1}{\sigma_i^2} \left[\frac{\partial v}{\partial x} - \frac{\partial v}{\partial x}(x_i) \right]^2 \right\} \qquad (2)$$

where $\frac{\partial v}{\partial x}$ are the theoretical tilts and $\frac{\partial v(x_i)}{\partial x}$ are the observed tilts. σ_i is the standard deviation of the data points. If the parameters in the theoretical tilt expression (1) are optimum, then the error defined by (2) will be a minimum. The variation of chi-square with each parameter in (2) describes a n-dimensional hypersurface (Bevington, 1969) the minmum of which can be found by setting the partial derivatives of chi-square with respect to each parameter, equal to zero:

$$\frac{\partial \chi^2}{\partial a_i} = \frac{\partial}{\partial a_i} \sum_{i=1}^{n} \left\{ \frac{1}{\sigma_i^2} \left[\frac{\partial v}{\partial x} - \frac{\partial v}{\partial x}(x_i) \right]^2 \right\} = 0 \qquad (3)$$

The set of simultaneous equations defined by (3) are in general highly non-linear and can be linearized by expanding in a Taylor's series (see for example Parrish and Gangi (1981) who use this method to determine thermoelastic constitutive equations for creeping halite), and then inverted (3) to find new parameter increments, da_i .

The minimum of the 8-dimensional hypersurface is approached using a search technique ,developed by Marquardt (1963). A typical search path using uncorrupted theoretical tilts for a fracture with parameters: (length x height x width) = 400 x 400 x .03 ft., azimuth = N35E, dip = 25 degrees SE, with well-head centered fracture coordinates appears in Figure 1. In this example, fracture depth is constrained at 3000 feet. The search for the optimum parameters is terminated when the change in chi-square from one iteration to the next is less than 0.1 percent. Fracture azimuth and dip are normally determined quite accurately after only a few iterations, while length, height, width, and fracture center coordinates converge more slowly to the correct values. The solution convergence rate depends on the proximity of the initial parameter, guesses to their values.

If the aforementioned theoretical tilts are corrupted, say by perturbing each tiltmeters' alignment with magnetic north by one degree, then an azimuth dip slice through the 7-dimensional (since depth is fixed) chi-square hypersurface produces an error contour map, which illustrates the solution convergence to the minimum (the minimum azimuth and dip is targeted at the " + " sign, Figure 2). The error in these maps is the mean square error (variance) and is equivalent to chi-square for $\sigma_i = 1$ in equation (2). Error units are in square microradians. The variation of chi-square with respect to azimuth and dip parameters is also illustrated in Figure 3. The theoretical and corrupted or "real" tilt vectors are overlain in a tilt vector map in Figure 4. Note that a one degree azimuth perturbation produces a nearly imperceptible change in the tilt field. The tilt components and site locations used to produce this map appear in Figure 5.

```
        -.1701[illegible]E-02          .9351[illegible]E-01 a b  0
         .3[illegible]E-01             .7402[illegible]E-01 a b  0
         .5[illegible]E-01             .3103[illegible]E-01 a b  0
         .446296E-01                  -.200846E-01 a b  0
         .439793E-03                  -.485994E-01 a b  0
        -.437[illegible]E-01          -.600074E-01 a b  0
        -.807[illegible]E-01          -.411212E-01 a b  0
        -.972[illegible]E-01          -.754922E-02 a b  0
        -.960[illegible]E-01           .242691E-01 a b  0
        -.835[illegible]E-01           .523891E-01 a b  0
        -.658[illegible]E-01           .756290E-01 a b  0
        -.469[illegible]E-01           .797165E-01 a b  0
         .271[illegible]E-02           .527376E-01 a b  0
        -.78[illegible]E-01           -.732657E-02 a b  0
        -.870[illegible]E-01           .455640E-01 a b  0
poissons ratio=     .25
frac. dimension (lxhxw)=    450.x    350.x    .035
azimuth and dip=          45.0       45.0
frac. depth=   3000.
well coordinates        25.       25.
location filename>a:anicr.loc
deltaa(j)
 .5000E+02  .5000E+02  .5000E-02  .3000E+00  .7000E-01  .5000E+02  .5000E+02
best-fit parameters:                                                          Iteration #
    length      height      thickness      az          dip          wc1          wc2
    377.395     307.740        .030       38.113      19.345      100.834     -133.861      1
chi-square     .27768E-03
sigmaa(j)
 .6030E+03  .4706E+03  .4707E-01  .1775E+00  .1760E+00  .2497E+03  .2440E+03
flamda=    .100000E-03

best-fit parameters:
    length      height      thickness      az          dip          wc1          wc2
    411.924     356.591        .033       31.409      27.366      -49.945       40.070      2
chi-square     .77000E-05
sigmaa(j)
 .3089E+03  .2499E+03  .2665E-01  .1369E+00  .6053E-01  .7382E+02  .7146E+02
flamda=    .100000E-04

best-fit parameters:
    length      height      thickness      az          dip          wc1          wc2
    389.364     375.629        .033       34.462      25.095       -4.791       -.938      3
chi-square     .14450E-06
sigmaa(j)
 .7745E+02  .6093E+02  .9260E-02  .9251E-02  .7494E-02  .9356E+01  .7589E+01
flamda=    .100000E-05

best-fit parameters:
    length      height      thickness      az          dip          wc1          wc2
    390.029     394.077        .031       34.999      25.036       -.866        .495      4
chi-square     .22976E-07
sigmaa(j)
 .6471E+02  .4300E+02  .6529E-02  .4193E-02  .4867E-02  .5965E+01  .4595E+01
flamda=    .100000E-06

best-fit parameters:
    length      height      thickness      az          dip          wc1          wc2
    399.329     399.510        .030       35.000      25.003       -.067        .047      5
chi-square     .44869E-08
sigmaa(j)
 .3810E+02  .2345E+02  .4694E-02  .1856E-02  .2731E-02  .3362E+01  .2031E+01
flamda=    .100000E-07

best-fit parameters:
    length      height      thickness      az          dip          wc1          wc2
    399.998     399.995        .030       35.000      25.000       -.001        -.001      6
chi-square     .77082E-13
sigmaa(j)
 .1604E+00  .9922E-01  .1879E-04  .7699E-05  .1171E-04  .1442E-01  .1082E-01
flamda=    .100000E-08

best-fit parameters:
    length      height      thickness      az          dip          wc1          wc2
    400.005     400.002        .030       35.000      25.000        .000        -.001      7
chi-square     .64830E-15
sigmaa(j)
 .1473E-01  .9111E-02  .1719E-05  .7054E-06  .1077E-05  .1326E-02  .9943E-03
flamda=    .100000E-09

best-fit parameters:
    length      height      thickness      az          dip          wc1          wc2
    400.005     400.002        .030       35.000      25.000        .000        -.001      8
chi-square     .64830E-15
sigmaa(j)
 .9068E-09  .9017E-09  .7153E-13  .4652E-11  .1856E-11  .2746E-08  .2784E-08
flamda=    .100000E+09

terminate search....change in chi-square < .1 % yfit(i)...predicted tilts
 -.373627E-01  -.179170E-02   .343678E-01   .545991E-01
  .446296E-01   .439802E-03  -.437035E-01  -.807811E-01
 -.972737E-01  -.960794E-01  -.835277E-01  -.658400E-01
 -.469785E-01   .271026E-02  -.780375E-01  -.870158E-01
  .910524E-01   .939175E-01   .740280E-01   .310339E-01
 -.200846E-01  -.485994E-01  -.600074E-01  -.411212E-01
 -.754922E-02   .242691E-01   .523891E-01   .756290E-01
  .797165E-01   .527376E-01  -.732650E-02   .455640E-01
```

Theoretical tilts for a fracture at
depth = 3000 ft.
length x height x width = 400 x 400 x .03 ft.
azimuth = N35E dip = 25 SE
fracture center coordinates at well-head.

Initial parameter guesses.

Figure 1. Typical search path using theoretical "uncorrupted" tilts as input.

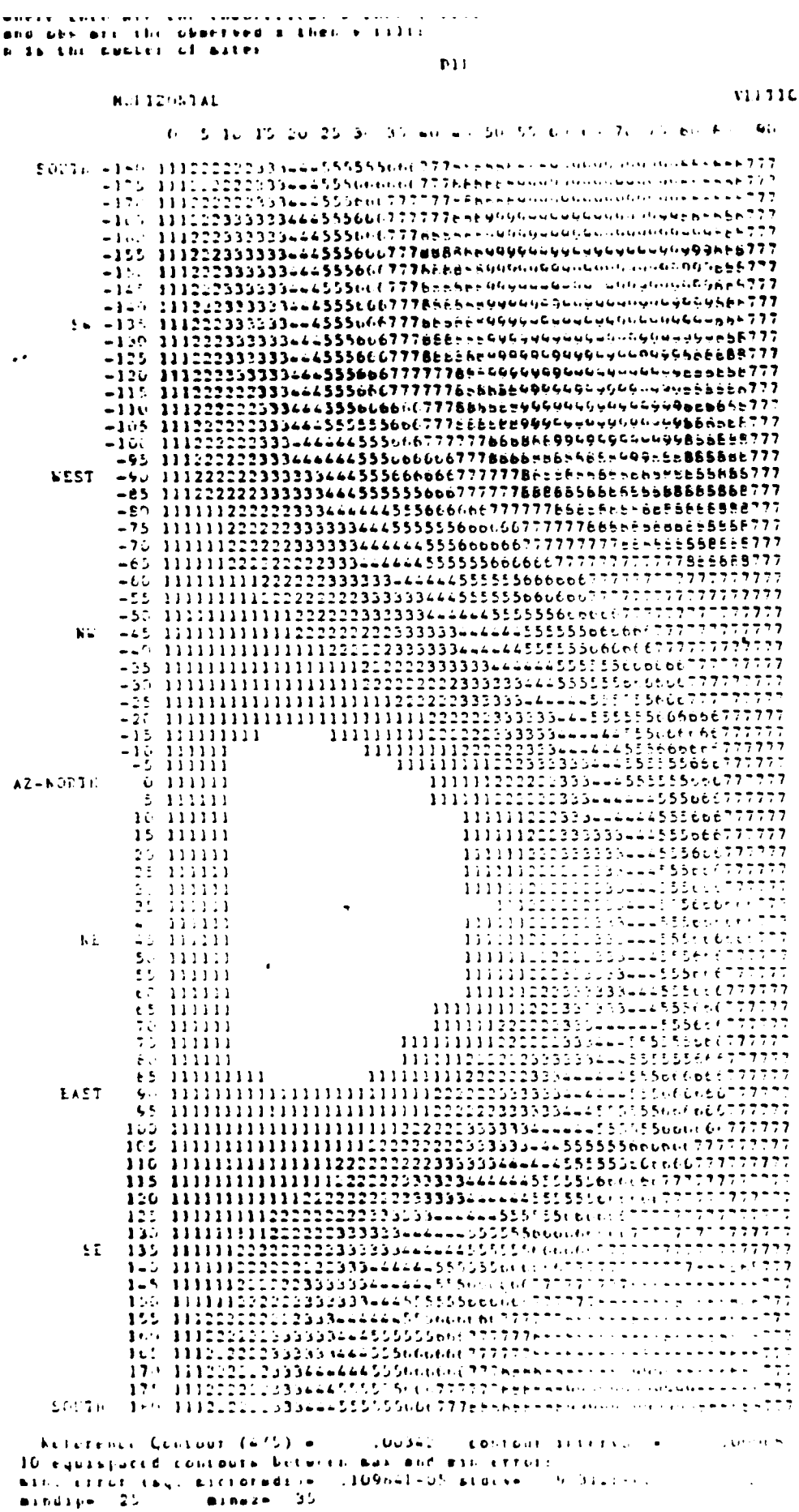

Figure 2. Error contour map in azimuth - dip space.

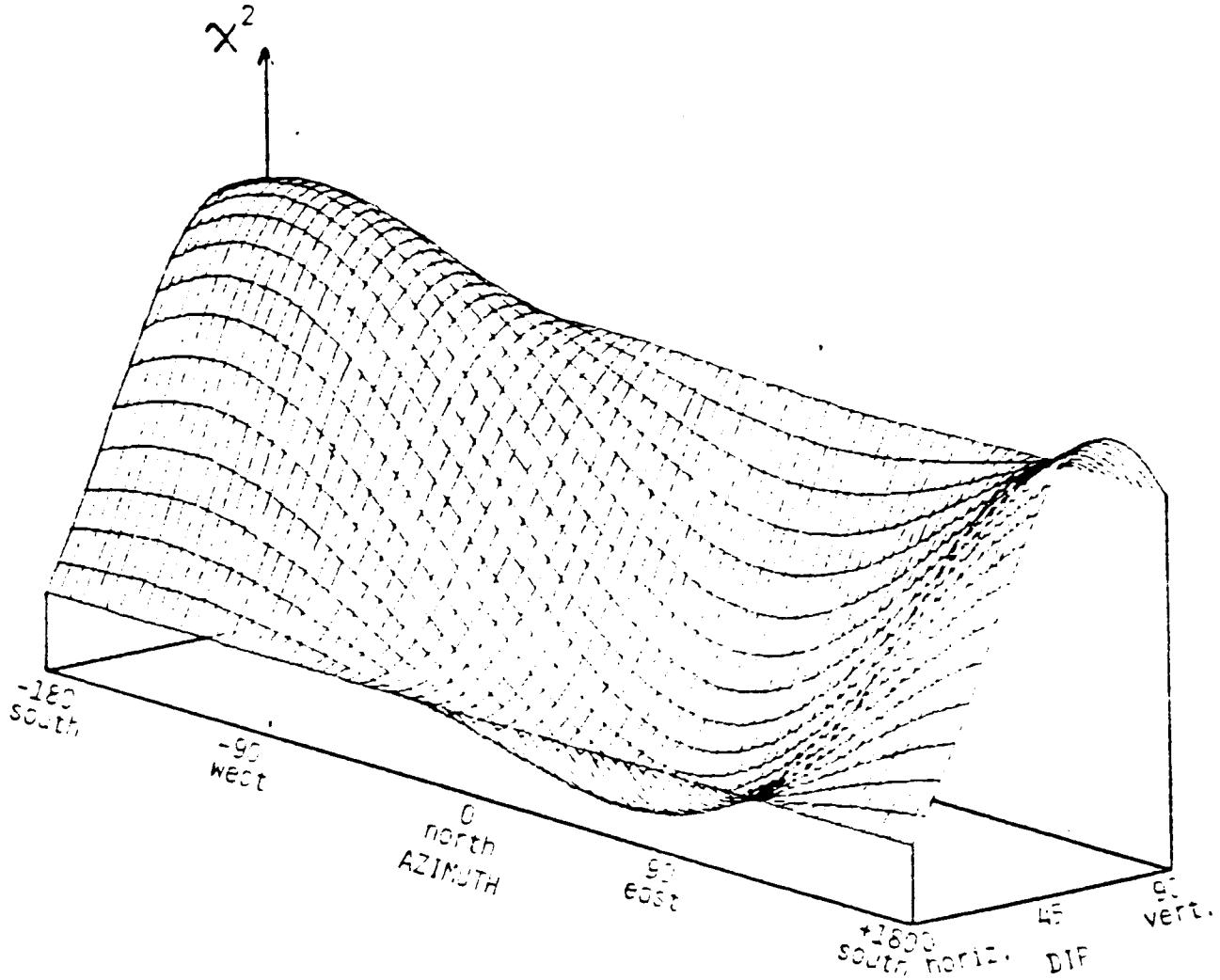

Figure 3. Variation of chi-square with azimuth and dip. Minimum at azimuth = N35E, dip = 25SE. see Fig. 2 for a contour map of this surface.

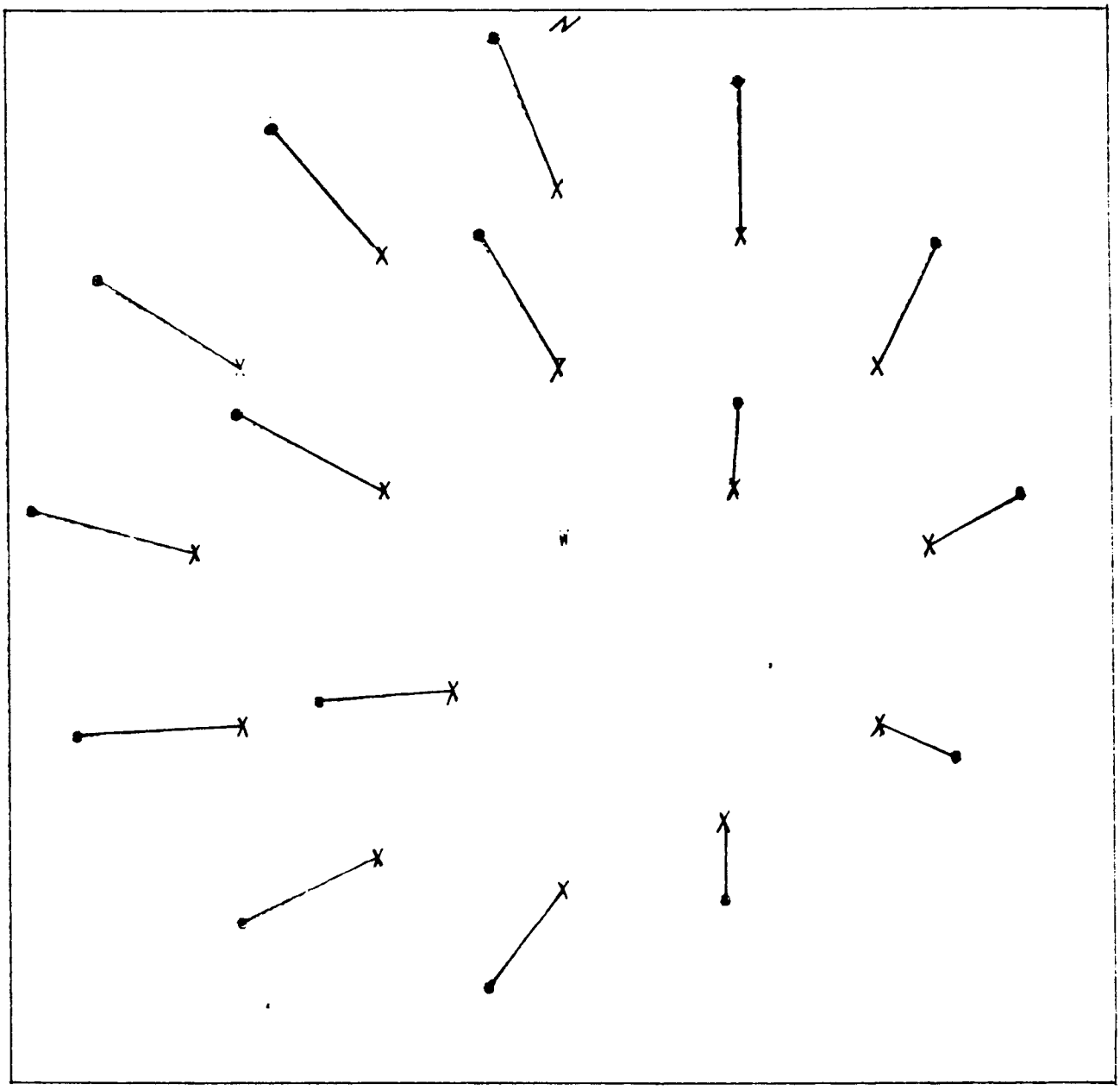

AZIMUTH: 35 deg
DIP: 25 deg
DEPTH: 3000 ft.

461 ft. per inch
.1 urad per inch
Theo
Real

Figure 4

Combined map of observed and modeled tilt vectors resulting from the injection of Well no. test on 6/6/86 lxhxw = 400x400x.03 ft.

THEORETICAL TILTS

```
-0.037362695201 47,0.09105228731889
-0.178677849920430E-02,0.09381746615009
0.03437071346954,0.07402986591461
0.05459909796064,0.03103380266071
0.04463351105711,-0.02009208092355
0.043880411621470E-02,-0.04867135840522
-0.04370358429995,-0.06000727747267
-0.08076764605184,-0.04116676507834
-0.09725689979269,-0.759058424097460E-02
-0.09606229322022,0.02425927016295
-0.08352499615352,0.05237554201745
-0.06585059021436,0.07561379015669
-0.04697851156456,0.07971647961653
0.275898935455610E-02,0.05273558463618
-0.07864571123356,-0.733236623227730E-02
-0.08765529654231,0.04555306328623
```

REAL TILTS

```
-0.03576792850027,0.09169050152019
-.00015408658709,0.09383448105983
0.03565453205126,0.07341692494288
0.05513239884819,0.03007618821942
0.04427227843885,-0.02086043474646
-0.040845014903390E-02,-0.04859967375473
-0.04474411710471,-0.05923552990958
-0.08148646066935,-0.03970511131716
-0.09739063722262,-0.585041073191400E-02
-0.09564121306654,0.02594221993663
-0.08260066320245,0.05383887997155
-0.06451006500084,0.07676654771 93
-0.04558010092985,0.08052424675045
0.363023491916500E-02,0.05268226769642
-0.07875338973902,-0.595304105838900E-02
-0.08680725496006,0.04708616659072
```

LOCATION.DAT

```
 16,1500
 0 , 1000
 499.7702 , 866.1581
 865.7599 , 500.4597
 1000 , 0
 866.5558 ,-499.0503
 443.5169 ,-765.8445
 1.528846 ,-959.9989
-495.3901 ,-866.953
-864.9619 ,-501.8277
-991.805 ,-19.67312
-867.3496 , 497.6993
-473.3797 , 814.4175
 0 , 500
 475.4295 , 154.8114
-293.119 ,-405.0695
-475.9205 , 153.2963
```

Figure 5. Tilt components and site locations in Fig. 4. Theoretical tilts are perturbed by altering declination of each instrument one degree, which creates "real" tilts.

REFERENCES

Bevington, P. R., 1969, Data Reduction and Error Analysis for the Physical Sciences, McGraw-Hill Book Co., New York, 336 pp.

Biot, M. A., Masse`, L., and Medlin, W. L., 1986, A two dimensional theory of fracture propagation, SPE Prod. Engng., Jan, p. 17-30.

Cleary, M. P., Kavvadas, M., and Lam, K. Y., 1983, Development of a fully three-dimensional simulator for analysis and design of hydraulic fracturing, SPE/DOE 11631 Joint Sympos. on Low Permeability Gas Res., Denver, Colorado, p. 271-282.

Davis, P. M., 1983, Surface Deformation Associated with a Dipping Hydrofracture, J. Geophys. Res., v. 88, p. 5826-5834.

Gazonas, G. A., 1985, The Mechanics of a Near-surface Crack under uniform pressure or shear in a transversely isotropic medium: with applications to hydraulic fracture, Ph.D. dissertation, Dept. of Geophysics, Texas A&M University, College Station, Texas, 191 pp.

Kanasewich, E. R., 1973, Time Sequence Analysis in Geophysics, Univ. of Alberta Press, Edmonton, Canada 352 pp.

Marquardt, D. W., 1963, An algorithm for least-squares estimation of non-linear parameters, J. Soc. Ind. Appl. Math., v. 11, p. 431-441.

Nolte, K. G., 1979, Determination of fracture parameters from fracturing pressure decline, SPE 8341, 54th technical conference, Las Vegas, Nevada, Sept.

Oppenheim, A. V., and Schafer, R. W., Digital Signal Processing, Prentice-Hall, Inc., Englewood Cliffs, New Jersey, 585 pp.

Parrish, D. K., and Gangi, A. F., 1981, A non-linear least squares technique for determining multiple mechanism, high-temperature creep flow laws, in: Mechanical Behavior of Crustal Rocks, Geophys. Monograph 24, The Handin Volume, AGU publ., Washington, D.C. 326 pp.

Pilant, W. L., 1979, Elastic Waves in the Earth, Elsevier Publ. Co., Amsterdam, The Netherlands, 493 pp.

Pollard, D. D. and Holzhausen, G. R., 1979, On the mechanical interaction between a fluid-filled fracture and the earth`s surface, Techonophys., v. 53, p.27-57.

Rice, J. R., and Cleary, M. P., 1976, Some basic stress diffusion solutions for fluid-saturated elastic porous media with compressible constituents, Rev. Geophys. Sp. Phys., v. 14, p. 227-241.

Smith, M. B., 1981, Stimulation design for short, precise hydraulic fractures - MHF, SPE 10313, 56th technical conference, San Antonio, Texas, Oct.

APPENDIX C

Tiltmeter Mapping and Monitoring of Hydraulic Fracture Propagation in Coal: A Case Study in the Warrior Basin, Alabama

Tiltmeter Mapping and Monitoring of Hydraulic Fracture Propagation in Coal: A Case Study in the Warrior Basin, Alabama

George A. Gazonas, Chris A. Wright and M. D. Wood[1]

ABSTRACT

Significant advances in the use of tiltmeter technology for hydraulic fracture mapping have been made during the past decade. Improvements have progressed in instrument design, site preparation, array processing to reject noise, and models for interpretation of the signal. These improvements have increased the precision of determining the orientation, dimensions, and positions of hydraulic fractures; they have also allowed the use of this technology in a greater variety of formations, at different depths, and at different rates and volumes of fracture treatments.

The relatively complex response of coal to hydraulic fracture stimulation makes real-time monitoring and mapping of the fracturing necessary. Real-time mapping provides timely information for comparison of fracture design with actual execution and offers an opportunity to modify the stimulation process as new conditions are revealed. Complex fracturing has been observed in a wide variety of materials as expected at shallow depths. The cleats (joints) of coal can enhance the overall tendency for discontinuities to compound the complexity of fracture response to stress gradients at shallow depths. The coal-cleat system may lead to pathologies, such as fracture growth out-of-zone and growth of a fracture out of the original plane. These induced fracture pathologies may deviate so far from actual design that dehydration of the slurry, leading to screenout and possible loss of the well, cannot be avoided unless a premonitory signal can be established in real-time data; such signals would allow steps to be taken to modify injection rates and slurry concentrations to mitigate risks.

A case study of a coal-bed fracture mapping job completed in Alabama is used to illustrate most of these points. In particular, a statistical test (F-test for the equality of variances) is used as a criterion for justifying an increase in source complexity when a single-fracture source does not adequately describe the observed surface-deformation field.

INTRODUCTION

Real-time mapping of hydraulic fracture stimulations in coal is of major importance in situations where job execution can deviate substantially from job design. Timely transmission of critical information can facilitate beneficial changes in injection parameters to minimize undesired results. It is the purpose of this paper to discuss general procedures, benefits, and risks associated with real-time fracture mapping. The discussion is not comprehensive but instead focuses on practical aspects of detection and description of what appears to be a widespread problem in hydraulic fracturing of coal—namely, generation of dual fractures during fracture stimulation.

No distinction is made between coal and other material in which this phenomenon has been observed. The discussion is restricted to a "blind" analysis of tilt data from an array of high-gain (nanoradian) surface tilt sensors and does not include the more realistic and desirable situation of integrated interpretation of treatment records and other reservoir data. The text is intended to be more of a descriptive real-earth discussion than an exhaustive theoretical discussion on each of the topics covered.

The first section of this paper outlines the theory and principles for tiltmeter hydraulic fracture mapping. The next section outlines a method for real-time monitoring of fracture growth with emphasis on detection of changes in fracture orientation. Finally, a case study is discussed which illustrates most of the major points outlined above.

[1] George A. Gazonas
Chris A. Wright
M.D. Wood
Hunter Geophysics
2344 Walsh Avenue, Building F
Santa Clara, California 95051

The work discussed in this paper includes results described in Hunter Geophysics' in-field reports on coal-seam hydraulic fracture mapping to C.M. Boyer II of United States Steel Corporation. The authors wish to thank the Rock Creek site personnel and GRI for their support of this project. The field work was subcontracted under GRI contract 5083-214-0847.

TILTMETER FRACTURE MAPPING

Theoretical Models

Theoretical displacement, tilt, and strain of the Earth's surface associated with seismic, volcanic, and other fracture sources is well established in the literature. Press (1965) discusses the dislocation modeling approach for seismic sources

and provides an extensive bibliography of other more basic dislocation modeling. The dislocation model herein employed is based on the Davis (1983) solution.

Theoretical models output surface deformations (solution to the forward problem) as a function of the source, or the subsurface fracture characteristics such as location, orientation, and dimensions of the source. The dislocation model presently being used has eight fracture-source parameters: dip, strike, length, width, height, depth, and the x and y positions of the fracture center relative to the wellbore. The theoretical deformations predicted by the model are relatively insensitive to the material properties of the medium and demonstrates its great utility for a variety of rock types.

Changes in source parameters produce changes in magnitude and direction of tilt at each site in a surface array of tiltmeters. This is the principle which allows a solution to the problem of determining source parameters from surface tilt measurements. If some knowledge of the surface tilt field is known, then solution of the inverse problem yields estimates of the source parameters. The method used to solve the inverse problem is discussed in a subsequent section.

Data Acquisition

An array of tiltmeters is installed in shallow (20 ft. deep) boreholes surrounding the injection well. Tilt response is uniformly sampled at all instrument locations. Solution precision is a strong function of quality of tilt data and the number of locations where tilt data are recorded.

Detection of high-resolution tilt requires an excellent detector and excellent coupling of the detector to the earth in a minimum noise environment (Wood and Allen, 1973). Commercial applications compromise these ideal observatory type characteristics. Instruments currently being used record tilt in two orthogonal directions. Signals recorded at each site are embedded in a broad spectrum of local, regional, solid earth tidal, meteorological, and planetary noise. It is therefore important to be able to obtain noise records prior to the start of the fracture treatment (injection) of sufficient duration to define the spectrum of noise.

In real-time applications, a background noise trend is least-squares fitted, using an appropriate model (Ljung, 1987), up to time of the injection. At that point, coefficients in the least-squares fit are fixed and are used to predict the noise trend during the time of injection. The signal is then defined as the difference between observed data and predicted noise trend. A signal tilt vector is then constructed for each site from the orthogonal signal channels at each site.

Fracture Solution

After obtaining a set of tilt vectors from an array of instruments, the goal is to determine the nature of the source that produced the observed tilt vectors. Using the dislocation model, a set of theoretical tilt vectors can be calculated at instrument locations for any given set of source parameters. Tilt is defined as the spatial derivative of the vertical displacement field (fig. 1). Graphically, the solution to source parameters is found when there is a best fit match between observed and theoretical tilt vectors (fig. 2).

The solution for source parameters that best fits the observed tilt field is obtained by a numerical minimization technique. An error functional is defined as the sum of the

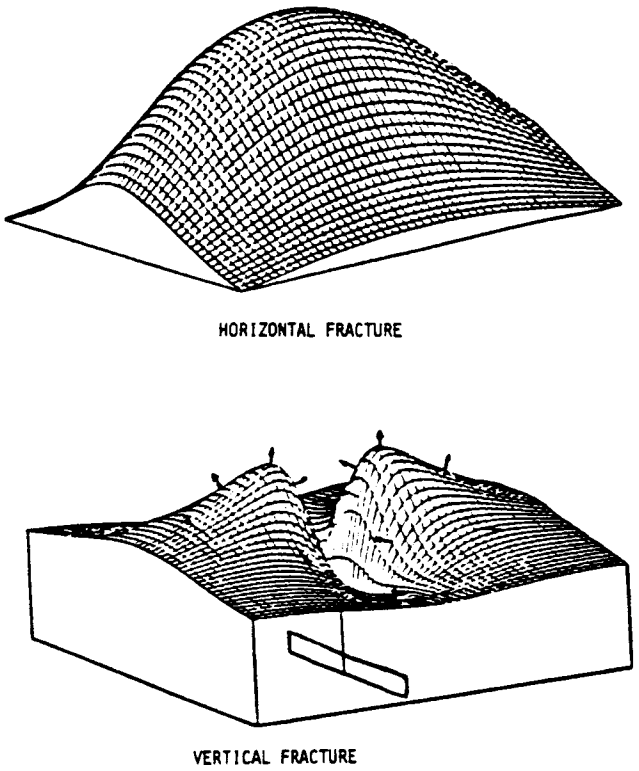

Figure 1. Vertical displacement fields induced above vertical and horizontal buried dislocations (adapted from Davis, 1983). Tilt is defined as the spatial derivative of the vertical displacement field.

squares of magnitudes of vector differences between observed and theoretical tilt vectors at each instrument location. The error functional, being a function of source parameters, is minimized by iterating over the possible range of source parameters. Ranges of possible source parameters can be constrained if specific information is known about the formation being stimulated or if conclusions can be drawn from other monitoring data (pressure analysis, temperature logs, radioactive tracers, etc.). Source parameters that give a minimum value of the error functional are considered best estimates of the actual fracture parameters.

It is important to simultaneously minimize the error functional with respect to all source parameters, rather than serially for each parameter, since the variation of the error functional for each parameter is dependent on the other parameters. The permutation of all possible combinations of eight parameters requires a practical assignment of the range and increment to be tested for each parameter and the rate of convergence that will give an acceptable computation time. The method of steepest descent facilitates these goals. This method is reviewed by Press and others (1986). It can be shown that this procedure will find the same minimum and is, therefore, equivalent to calculation of all possible permutations of values for the same parameters, if the error surface is "smooth" to at least second order derivatives. The procedure is rapid and output is the optimum value and local convergence sensitivity for each parameter.

It is illustrative to obtain slices through the 8th order error surface to show the relative behavior of convergence to the

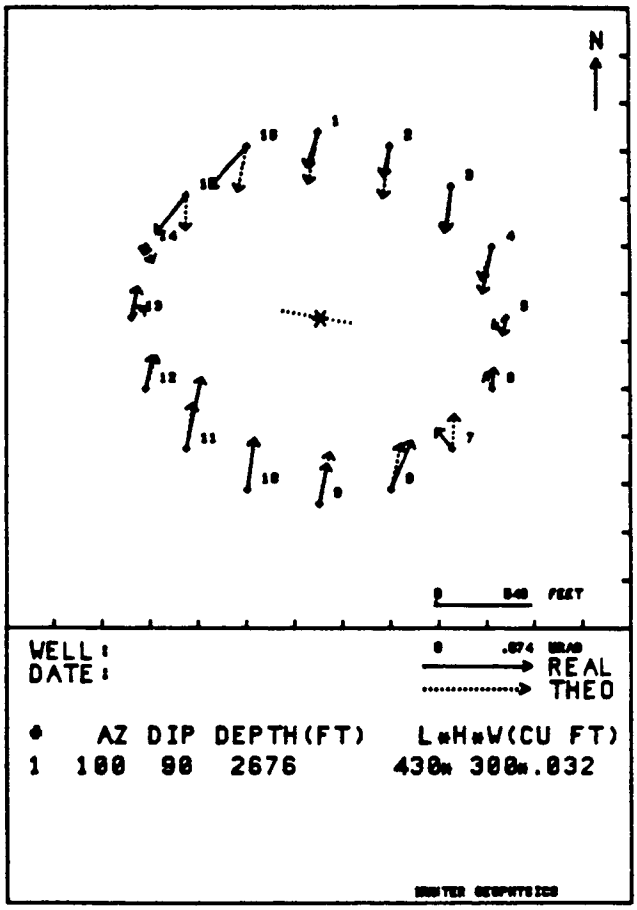

Figure 2. Overlay of observed (solid lines) and theoretical (dotted lines) tilt vectors for a vertical hydraulic fracture and the associated fracture solution (depicted by the dotted line through the wellbore).

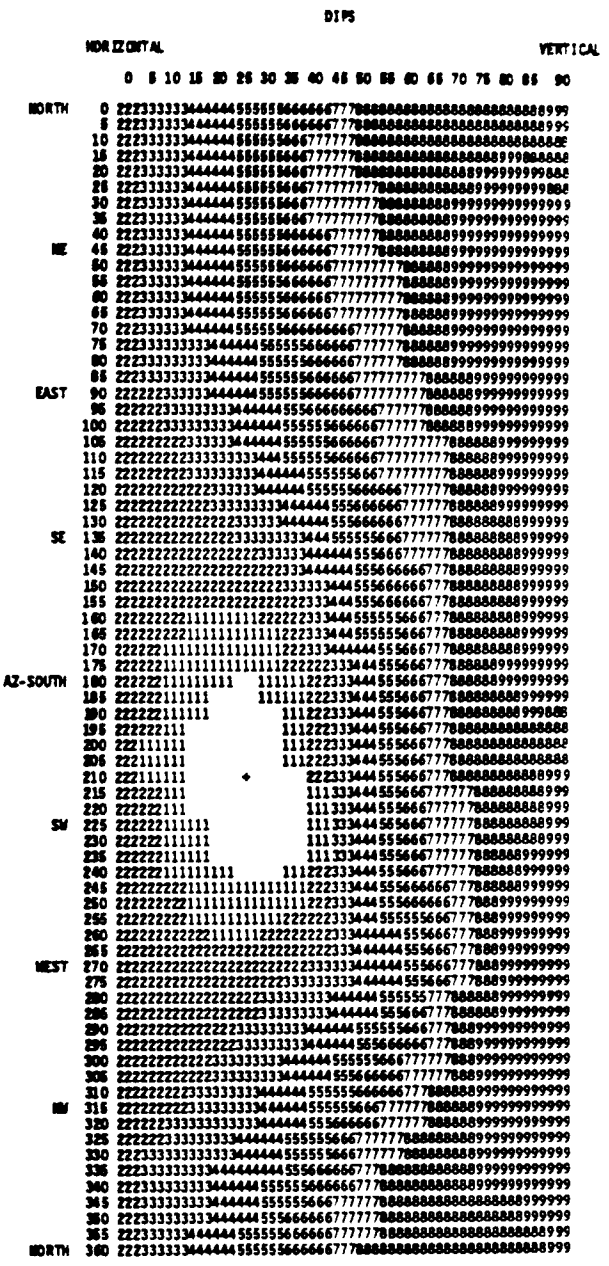

Figure 3. Contoured error surface for the P1A stimulation in azimuth-dip space. The surface is obtained by fixing all other fracture parameters and calculating the mean-squared error between observed and theoretical tilts at 5 degree increments in orientation over all sites. The minimum error occurs at the + sign at azimuth N. 30 E. and dip 25 northwest. Subsequent logarithmic contours are depicted by the number 1 through 9 in the plot.

best solution for each parameter. The error surface for orientation is useful to present as an error matrix of dip vs. strike (fig. 3). The error function for volume is obtained by varying fracture dimensions while keeping all other parameters fixed (fig. 4). Illustrations such as these assist in visualizing the convergence to the best fit obtained from the eight-dimensional method of steepest descent.

The model has highest sensitivity to orientation of the fracture. Azimuth and dip of a fracture can usually be precisely determined. The magnitude of the tilt signal is proportional to source volume and inversely proportional to the cube of the source depth. The least sensitivity of the model is to the linear dimensions of the fracture or how the fracture volume is partitioned. Volume partitioning between width and area is much more sensitive than partitioning of the area between height and length.

Complex Fractures

In some cases the error functional minimization yields a solution that still has a significant error between observed and theoretical tilt vectors. This can occur due to a very low signal-to-noise ratio, where there is great uncertainty in measuring the surface tilt field. In cases where expected tilt-signal magnitudes are very small or environmental noise is extremely high across the whole array, the solution for fracture source parameters may not be possible. In the case of poor fit due to poor signal-to-noise ratios, tilt error vectors will represent, by definition, noise. There is, however, another possible scenario.

Array processing techniques can determine whether a group of error vectors across an array are in some fashion coherent, spatially low frequency, or are spatially random (measurement noise). Details of this are omitted due to complexity of the

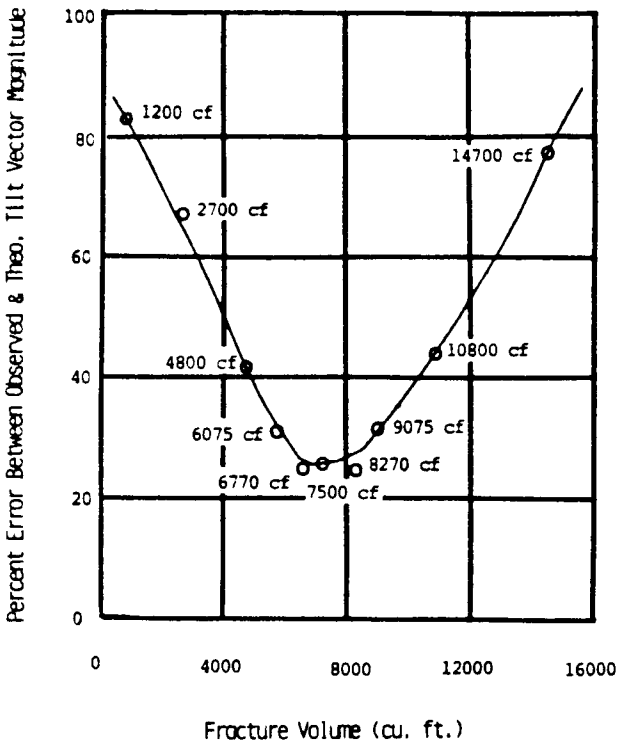

Figure 4. Parabolic error surface of the mean-squared error versus volume obtained by varying the dimensions of the single fracture and keeping all other fracture parameters fixed.

argument. The result is that in some cases high residual errors at the end of a best-fit minimization are not due to poor data quality but instead are due to insufficient model accuracy. In these cases, the remaining error vectors are not random, but display a regular pattern across the array. Experience has shown that if the single fracture model is expanded to include more complex fracture structures, then a quality of fit more commensurate with observed signal-to-noise ratio is possible. It has been found that fracture growth can change in orientation during a stimulation, or even grow in two planes simultaneously.

More than 1,000 fracture jobs have been monitored with tiltmeters with the bulk of them executed at depths of less than 3,000 feet within the past 48 months. A very large percentage of these jobs indicate that fracture complexity is far more widespread than is commonly acknowledged. The role of stress in determining fracture orientation is well established. Fracture stimulations alter the magnitude of principal stresses and in those cases where the difference between the intermediate and least principal stress is reversed in sense, incremental fracture growth will occur out of the original fracture plane. When fracture growth breaks out in another plane, (documented instances can be found in Evans and others, 1982; and Smith and others, 1985) often times there is an abrupt change in slope on the raw tiltmeter records on all (or many) channels in the array. The abrupt slope break can be detected and interpreted in real-time to indicate if and when fracture growth initiates in a second plane. In some instances, however, abrupt slope changes are not present on the raw tilt records, yet alternative evidence clearly indicates that a multiple fracture system has developed. This can occur in formations where the in-situ principal stresses do not appreciably vary with depth, or when one fracture component is significantly larger than the other. This paper discusses a simple but widespread condition of fracture growth in more than one plane to illustrate the value of real-time fracture mapping.

Real-time Monitoring of Fracture Growth

Real-time mapping of hydraulic fracturing is valuable in those operations that can deviate substantially from fracture design and possibly lead to pathologies such as screenout and loss of a well. Fracture complexity such as out-of-zone growth, growth in an orientation other than the original design, growth out of a single fracture plane leading to dual fractures, and unexpected leakoff are serious deviations from fracture design that surface tilt measurements are especially sensitive to. In many of these situations it may be possible to recognize premonitory conditions that can be altered by changes in injection rates and slurry concentrations to recover control sufficiently to produce a more desirable result, even if the original design cannot be restored. A grid of high resolution tilt sensors can contribute basic information, which together with other real-time data, serves to constrain the interpretation of each output parameter to a useful result.

Fracture growth in two planes, especially in orthogonal planes, can seriously threaten the successful completion of a stimulation. Difference in fracture aperture between a vertical and a horizontal fracture can cause dehydration of the slurry in one fracture, leading to premature screenout at undesirable locations in the fracture system. Screenout is not an instantaneous process, and if tilt sensors can detect the onset of new fracture growth out of the single plane of the fracture before dehydration causes bridging and screenout, options can be preserved for job completion.

Tilt vectors are quite sensitive to changes in orientation of new fracture growth. A horizontal fracture will have a fourfold greater leverage on the free surface (i.e. tilt signal) than a vertical fracture of the same volume and surface area at the same depth. Moreover, given the inverse cube relation of signal amplitude with depth, tilt is a sensitive detector of changes in orientation and depth. Thus, out-of-zone growth and growth out of a single fracture plane are pathologies that tilt data can address in real-time.

Changes in fracture orientation can appear on raw tilt records as abrupt changes in slope, or time-rate of change-of-tilt. If a fracture grows in a vertical plane and then changes orientation and some fraction, or all, of the injected fluid starts to flow into a horizontal fracture plane, the output slope of tilt data can change (fig. 5). The complex fracture propagation process can then be analyzed by temporally partitioning the tilt data (fig. 6).

For the first part of the job, the fracture was clearly oriented vertically, and for the latter part of the job, the fracture changed to a horizontal orientation. By the time of shut-in, the tilt component due to the horizontal fracture had almost entirely swamped the vertical tilt component. In fact, the fracture may have been diagnosed as horizontal if one only looked at orientation of tilt vectors at completion of the injection. Both the abrupt slope change, which was seen on all channels, and the resulting volume discrepancy point to the creation of a complex fracture structure. Real-time analysis is

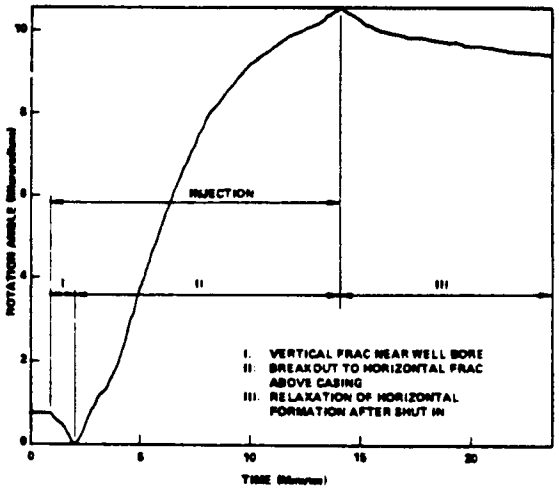

Figure 5. Three stages of fracture formation (from Wood and others, 1983).

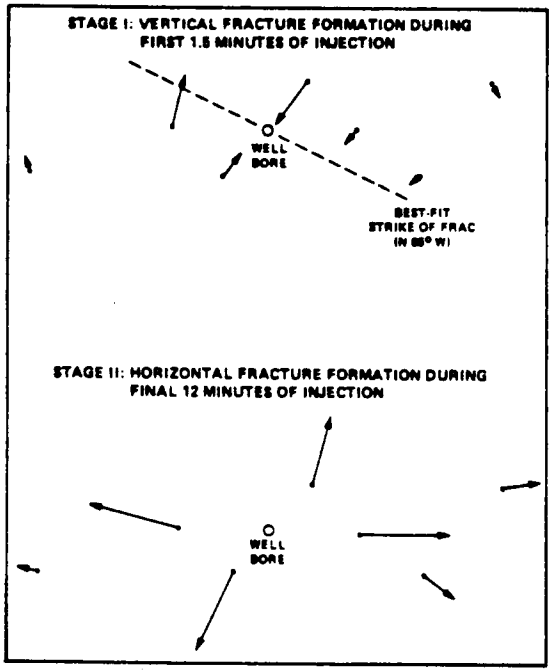

Figure 6. Measured tilt profiles during stages I and II of fracture formation (from Wood and others, 1983).

a type of path-dependent analysis that helps to resolve such ambiguities.

A real-time monitoring system would interpret a change in slope of tilt data across the whole array of instruments as a change in fracture orientation or fracture growth rate. If only one instrument had an abrupt slope change, this could be diagnosed as noise since it was not seen across the whole array. Once a change in orientation is detected, the fracture model would expand to include complex fractures, and monitoring would continue, unless it was decided to cease injection or modify treatment parameters.

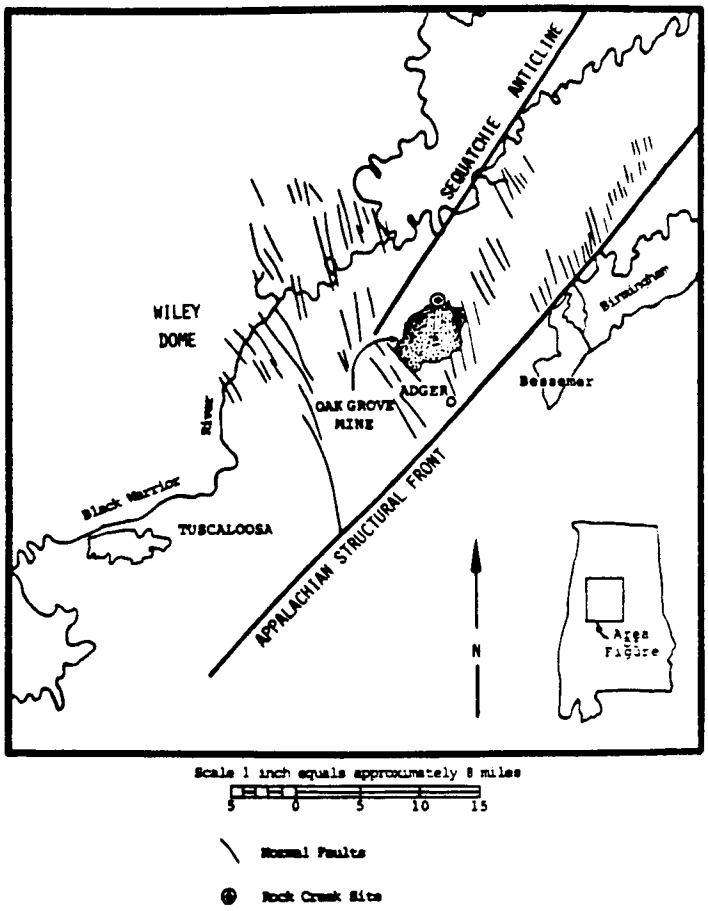

Figure 7. Map showing the location of the Rock Creek site and regional geologic structure of the southeastern Warrior Basin (redrawn from Camp and others, 1985).

COAL-BED FRACTURE MAPPING: A CASE STUDY

Geologic Setting

The Rock Creek site is located approximately 15 miles west of Birmingham, Alabama within the Warrior Basin and is bounded on the west by the Sequatchie Anticline and on the east by the Appalachian fold and thrust belt (fig. 7). The Warrior Basin of Alabama and Mississippi is structurally much less deformed than the Appalachian fold and thrust belt although numerous northwest-striking normal faults appear to be related to the Appalachian orogeny. Strata at the site reside within the Coalburg syncline and dip less than one degree to the south. Multiple coal seams at the Rock Creek site are in the Lower Pennsylvanian Pottsville Formation and primarily consist of interbedded sandstones, siltstones, and shales (Camp and others, 1985). Oriented cores were taken from monitor wells M1A (Pratt Group at 480 feet), M1B (Mary Lee Group at 1,050 feet), and M1C (Black Creek Group from 1,250 to 1,440 feet) (fig. 8). These coal groups contain an orthogonal set of joints; a preponderance of the face cleats have an average trend of N. 61 E. and butt cleats with an average trend of N. 142 E. (fig. 9).

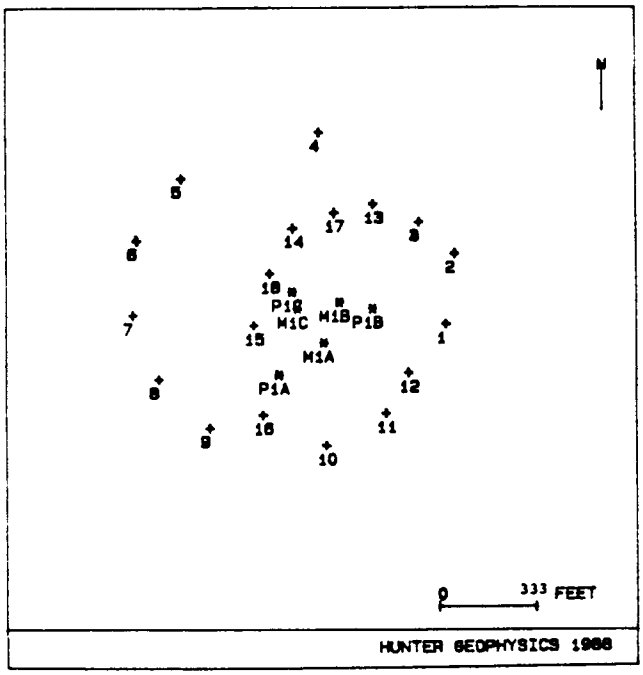

Figure 8. Map showing the location of monitor wells M1A, M1B, M1C; production wells P1A, P1B, P1C; and 18 tiltmeter sites.

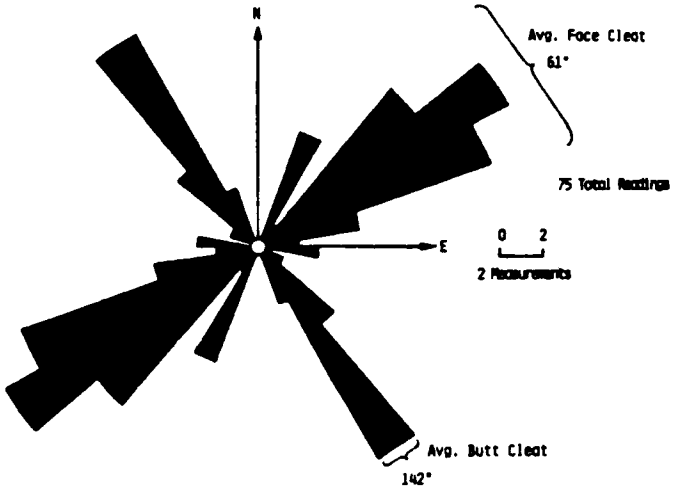

Figure 9. Composite rose diagram of average face and butt cleat orientations measured from oriented cores taken from monitor wells M1A, M1B, and M1C (redrawn from Boyer and others, 1984).

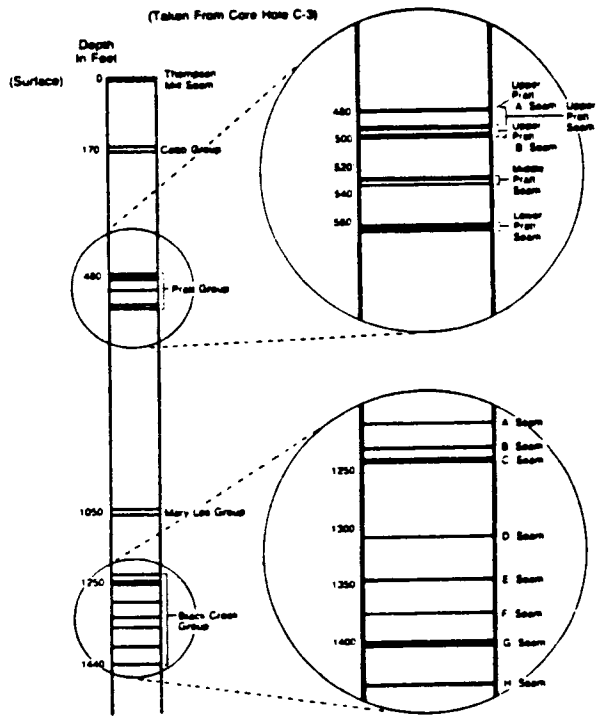

Figure 10. Stratigraphic column of Rock Creek site coals (from Schraufnagel and others, 1987).

Coal Seam Stimulations

Three hydraulic-fracture stimulations were performed in multiple coal seams at the GRI/USX Rock Creek site in June and July of 1986. Methane production wells P1A, P1B, and P1C were stimulated at depths which ranged from 480 feet to 1,500 feet in the Pratt, Mary Lee-Blue Creek, and Black Creek coal groups (fig. 10). The stimulations consisted of a water prepad followed by a gel pad and a sand-laden cross-linked gel (Nielsen and Hanson, 1987). Injection rates ranged from 15 to 20 barrels per minute (bpm). Willis and others (1987) give a summary of fluid rheologies, pressures, and rates employed on these jobs. In addition, their paper provides the results of a fracture simulator which outputs in real-time, estimates of fracture dimensions, net fracture pressure, and treatment pressure. However, the precision in their estimates of fracture parameters is not given in their paper.

In a subsequent section, we summarize the results of a geophysical inversion technique which provides estimates, as well as the precision in the estimates, of fracture-source parameters. The accuracy in the predictions of modeling efforts can only be verified with direct observation of the fracture (for example with mine-back experiments).

Tiltmeter Measurements

Hunter Geophysics installed an array of 18 tiltmeters around wells P1A, P1B, and P1C in a configuration designed to optimize the expected tilt signals for each of the three stimulations (fig. 8). Maximum theoretical surface tilts for both horizontal and vertical fractures in the opening mode occur at a radial distance from the injection point which is equal to about 40 percent of the depth to the fracture center. Tilt data were continuously recorded at a rate of one sample per minute from a day before each stimulation until a few hours after shut-in of the wells. A re-analysis of the tilt data for each stimulation corroborates the results that were obtained in the in-field analyses. The fracture source parameter solutions and total-tilt vectors (accumulated from breakdown to shut-in) for each stimulation appear in figures 11a, 11b, and 11c.

The surface tilts which resulted from the stimulations created signals that were much larger than the resolution limits of the tilt sensor (5 nanoradians). Tilt amplitudes for the total injection interval (accumulated from formation breakdown to

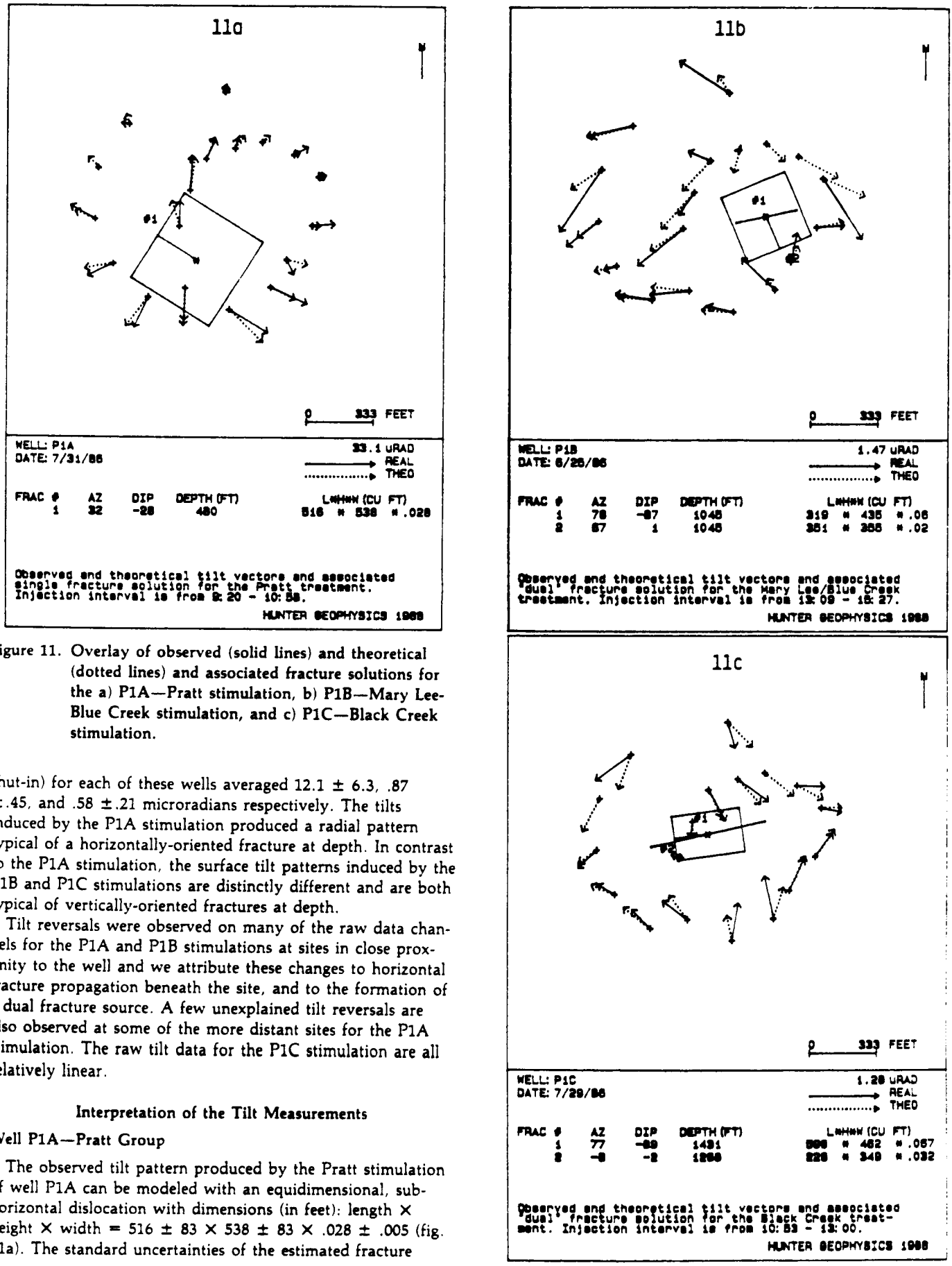

Figure 11. Overlay of observed (solid lines) and theoretical (dotted lines) and associated fracture solutions for the a) P1A—Pratt stimulation, b) P1B—Mary Lee-Blue Creek stimulation, and c) P1C—Black Creek stimulation.

shut-in) for each of these wells averaged 12.1 ± 6.3, .87 ±.45, and .58 ±.21 microradians respectively. The tilts induced by the P1A stimulation produced a radial pattern typical of a horizontally-oriented fracture at depth. In contrast to the P1A stimulation, the surface tilt patterns induced by the P1B and P1C stimulations are distinctly different and are both typical of vertically-oriented fractures at depth.

Tilt reversals were observed on many of the raw data channels for the P1A and P1B stimulations at sites in close proximity to the well and we attribute these changes to horizontal fracture propagation beneath the site, and to the formation of a dual fracture source. A few unexplained tilt reversals are also observed at some of the more distant sites for the P1A stimulation. The raw tilt data for the P1C stimulation are all relatively linear.

Interpretation of the Tilt Measurements

Well P1A—Pratt Group

The observed tilt pattern produced by the Pratt stimulation of well P1A can be modeled with an equidimensional, sub-horizontal dislocation with dimensions (in feet): length × height × width = 516 ± 83 × 538 ± 83 × .028 ± .005 (fig. 11a). The standard uncertainties of the estimated fracture

parameters are determined by the method described by Press and others (1986). The fracture strikes N. 32 E. ± 11, and dips 28 ± 7 degrees northwest. Tilt data from sites 6 and 13 were deleted from the inversion data set since a large percentage of the solution error could be attributed to the mismatch between observed and theoretical tilt vectors for these sites. In addition, the fracture center is fixed at the wellbore and the fracture depth is fixed at the injection depth (approximately 480 feet). The solution provided is the best in a least squares sense and can be visualized in azimuth-dip space with a mean square error plot (fig. 3). The minimum error occurs at the + sign with subsequent logarithmic contours depicted by the numbers 1 through 9 in the plot.

Several attempts to model the observed tilt vectors using a more complex dual fracture source (a source consisting of both vertical and horizontal fracture components) did not significantly reduce the overall solution error. In fact, the ratio of the mean square errors (variances) for the dual and single fracture solutions is near unity, and hence there is no justification based on tilt data alone to increase the source complexity by admitting a vertical fracture component in the solution. The question as to whether a dual fracture solution is significantly better than a single fracture solution can be evaluated with an F-test for the equality of variances. In order to test for the equality of variances we can form the statistic F = var1 var2 which follows an F-distribution (Mendenhall, 1975). In this equation, the quantities var1 and var2 are the solution-error variances, or the mismatch between observed and theoretical tilt vectors, for the dual and single fracture solutions, respectively. Tabulated values of the F-distribution for various significance levels and degrees of freedom are obtainable from most introductory statistic textbooks.

Nielsen and Hanson (1987), incorporating pressure and well-logging data, provide an alternative interpretation of the tilt data with a solution that admits both vertical and horizontal fracture components. In their solution, the vertical fracture trends N. 73 E. and consists of less than 10 percent of the total injected slurry volume. The horizontal fracture comprises greater than 90 percent of the total fracture volume and has migrated up dip and to the northwest by approximately 110 feet. The method used to solve the inverse problem is not given in Nielsen and Hanson (1987), nor is any reference made to the precision of their estimates of the fracture source parameters. Willis and others (1987) provide real-time predictions of fracture length and net fracture pressure for the P1A stimulation, yet the precision in their estimates of the fracture parameters is not provided in their paper. In addition, their formalism is not general enough to provide precise estimates of fracture orientation.

It is interesting to note that gamma ray and acoustic televiewer logs reveal the presence of two vertical wellbore fractures in the Upper Pratt coal seams, yet there is no evidence of horizontal fractures in these seams. This could be attributed to the tools' inability to differentiate between the acoustic properties of a sand-filled horizontal fracture and partings in the coal seams. The orientations of the vertical fractures as determined by the acoustic logs is N. 78 E. and N. 93 E.; the fractures are oblique to the butt and face cleat orientations (fig. 9). Our analysis of the tilt data indicate that it is likely that the vertical fractures were limited to the vicinity of the wellbore and acted as fluid conduits to the dominant horizontal fracture that was created during the stimulation. Further evidence for the presence of horizontal fractures in the Pratt group comes from the results of in-situ stress measurements in well M1A. The measurements indicate that horizontal fractures can form in the Pratt group, at depths of 480 feet, after only 15 gallons of water are injected (at 5-6 gpm) into the formation, since fracture re-opening pressures during successive injection cycles are nearly equal to the overburden stress (Boyer and others, 1985). Hydraulic stimulation at greater depths in adjacent wells P1B and P1C created vertical fractures which volumetrically contributed 77 and 88 percent, respectively, to the total fracture volume.

Well P1B—Mary Lee-Blue Creek Group:

The observed tilt pattern produced by the Mary Lee-Blue Creek stimulation of well P1B can be modeled by a dual fracture source with a vertical component with dimensions (in feet): length × height × width = 319 ± 269 × 435 ± 238 × .060 ± .066. The vertical fracture component strikes N. 78 E. ± 4.5, and dips 87 ± 2 degrees northwest. One might have expected the azimuth of the vertical fracture to parallel either the butt or face cleat orientations in the coal (fig. 9). However, mining back into hydraulically induced fractures in coal has shown that the fractures have a stair-step pattern and follow oblique orientations, relative to butt and face cleat orientations (Diamond, 1987). The horizontal fracture component has dimensions (in feet): 351 ± 278 × 355 ± 282 × .020 ± .021. The horizontal fracture azimuth is N. 67 E. ± 360 and dips 1 ± 7 degree southeast (fig. 11b). The large standard uncertainty in fracture azimuth is expected, since azimuth becomes undefined as the fracture dip approaches zero. The standard uncertainties in fracture orientation are normally within 5 degrees. Tilt data from sites 3 and 13 were deleted from the inversion data set because a large percentage of the solution error could be attributed to the mismatch between observed and theoretical tilt vectors for these sites. In addition, both fracture centers are fixed at the wellbore and the fracture depths are fixed at the injection depth (approximately 1,045 feet). The vertical fracture component contributed 77 percent of the total modeled fracture volume. Additional evidence for the existence of complex fracture geometries in coal has been confirmed with direct observation of the fractures in mine-back experiments (Diamond, 1987).

The observed tilt vectors were initially inverted using a single fracture source model. The residual error was relatively large and the inversion proceeded by assuming a dual fracture source model. The ratio of solution error variances improved by a factor of 2.1, which is statistically significant at the 95 percent confidence level. A comparison of figures 11a and 11b illustrates the distinctive change in the surface tilt pattern with the introduction of a vertical fracture component.

Well P1C—Black Creek Group

The observed tilt pattern produced by the Black Creek stimulation of well P1C can be modeled by a dual fracture source with a vertical component with dimensions (in feet): length × height × width = 598 ± 245 × 462 ± 165 × .067 ± .026. The vertical fracture component strikes N. 77 E. ± 2.3, and dips 89 ± .6 degrees northwest. The horizontal fracture component has dimensions (in feet): 228 ± 135 × 349 ±

202 × .032 ± .018. The horizontal fracture azimuth is N. 8 W. ± 108 and dips 2 ± 3.8 degrees southwest (fig. 11c). Tilt data from sites 6 and 13 were deleted from the inversion data set since a large percentage of the solution error could be attributed to the mismatch between observed and theoretical tilt vectors for these sites. In addition, the fracture center depth for the vertical component is fixed at the injection depth (1,431 feet) and the fracture depth for the horizontal component is fixed at 1,268 feet. The vertical fracture component contributed 88 percent of the total modeled fracture volume.

The observed tilt vectors were initially inverted (as for the P1B stimulation) using a single fracture source model. The residual error was relatively large and the inversion proceeded by assuming a dual fracture source model. The ratio of solution-error variances improved by a factor of 4 (even though the horizontal component only contributes 12 percent of total volume), which is statistically significant at the 95 percent confidence level, and so we are justified in admitting the more complex fracture source model.

SUMMARY and CONCLUSIONS

The outline provided in this paper of tiltmeter fracture-mapping technology and the specific discussion of three separate stimulations in a coal formation demonstrate how it is used to obtain valuable real-time information of fracture-source parameters. Although the existing tiltmeter mapping is not optimized and is continually improving, it has been successfully applied to several hundred jobs in tar sands, diatomite, shale, and coal.

The geophysical inversion of surface tilt data provides estimates, as well as standard uncertainties, of fracture source parameters which include fracture azimuth, dip, depth, fracture center coordinates, and fracture dimensions which include length, height and width. The solution of the inverse problem using synthetic tilt data is unique, and since real data is contaminated with noise, the solution for fracture parameters often provides only fuzzy estimates of fracture dimensions. The standard uncertainties of the estimated azimuth and dip of single and dual fracture structures are usually within five degrees, whereas fracture dimensions are less precisely determined. However, given the sensitivity of tilt data to overall volume change, and the general condition that fracture closure following shut-in involves width changes with relatively little change in length or height, estimates of area and width can be made with models that also admit pressure data. Moreover, using pressure data to distinguish confined height versus length from area is determined by tilt with a model that jointly inputs pressure, rate, and tilt data.

Three hydraulic fracture stimulations were performed in multiple coal seams at the GRI/USX Rock Creek site in June and July of 1986. Methane production wells P1A, P1B, and P1C were stimulated at depths of 480 feet, 1,045 feet, and 1,431 feet, respectively, in the Pratt, Mary Lee-Blue Creek, and Black Creek coal groups. Fracture source parameters for each of the stimulations were obtained using geophysical inversion techniques. The tiltmeter data indicate that dual fracture sources (vertical and horizontal components) are required to best-fit the observed tilt patterns induced by the two deeper stimulations in the P1B and P1C wells. The direct observation of T-shaped fractures in the Blue Creek coal seam at USX's Oak Grove mine (Diamond, 1987) supports our interpretation for the creation of dual fractures during the P1B stimulation. The vertical fracture azimuths were found to trend approximately N. 78 E. and at oblique angles to the face cleat orientations (N. 61 E.) observed in oriented cores taken from adjacent monitor wells. An independent interpretation of the tilt data by Nielsen and Hanson (1987) essentially corroborates our interpretation for the creation of dual fractures during the P1B and P1C stimulations.

Inversion of the observed tilts induced by the stimulation of the shallowest P1A well revealed the presence of a large sub-horizontal fracture. Vertical fractures may have formed as a result of the stimulation but are volumetrically insignificant. Additional evidence for the presence of horizontal fractures and limited vertical fractures in the Pratt group comes from the results of in-situ stress measurements in well M1A. Pressure data indicate that horizontal fractures form through rollover after only 15 gallons of water are injected into the formation, since fracture re-opening pressures during successive injection cycles are nearly equal to the overburden stress (Boyer and others, 1985).

Gamma ray and acoustic televiewer logs revealed the presence of two vertical wellbore fractures in the Upper Pratt coal seams yet there is no evidence of horizontal fractures in these seams. This could be attributed to the tools' inability to distinguish between a horizontal sand-filled fracture and partings in the coal seams. The orientations of the vertical fractures as determined by the acoustic logs are N. 78 E. and N. 93 E., and they are oblique to the butt and face cleat orientations in the coal. Our analysis of the tilt data indicates that it is likely that the vertical fractures were limited to the vicinity of the wellbore and acted as fluid conduits to the dominant horizontal fracture that was created during the stimulation.

Further evidence for the absence of a significant vertical fracture component in the Pratt group is supported by the observation that post-stimulation methane production is poorest in the P1A well, although relatively low initial reservoir pressures could also explain this phenomenon (Schraufnagel and others, 1987). If our interpretation is correct, alternative stimulation designs should be developed which contact more of the seams in the shallow Pratt group.

The determination of fracture-source parameters by any method should include the precision of the estimated parameters. A precise comparison of the values of the same source parameter provided by different methods (seismic, borehole televiewer, and other logging data) was severely limited in this paper by the failure to provide, in the references cited, values for the precision in the estimated parameters. Non-uniqueness is a fact of inversion for the study of physical processes that are remotely sensed. No single geophysical tool will give equal quality determinations of source parameters; therefore, the trend of future analyses will be to integrate the determinations from a variety of complementary tools to constrain the solution to the least-error, most plausible condition. Inverting these data with a more comprehensive real-earth model of the processes will then be justified.

REFERENCES CITED

Boyer, C. M., II, Briscoe, F. H., Camp, B. S., Dobscha, F.X.,

Malone, P.G., Militzer, M.R., and Stubbs, P.B., 1984, Rock Creek methane from multiple coal seams completion project: Gas Research Institute Quarterly Report, November-January.

Boyer, C.M., II, Briscoe, F.H., Camp, B.S., Dobscha, F.X., Hirko, N.M., Malone, P.G., Militzer, M.R., Pavone, A.M., Schwerer, F.C., and Stubbs, P.B., 1985, Rock Creek methane from multiple coal seams completion project: Gas Research Institute Quarterly Report, May-July.

Camp, B.S., Briscoe, F.H., Malone, P.G., and Boyer, C.M., II, 1985, Rock Creek methane from multiple coal seams completion project, *in* Special data package preliminary geologic report: Gas Research Institute, Chicago, Illinois.

Davis, P.M., 1983, Surface deformation associated with dipping hydrofracture: Journal of Geophysical Research, v. 88, no. 87, p. 5826-5834.

Diamond, W.P., 1987, Characterization of fracture geometry and roof penetrations associated with stimulation in coalbeds, *in* Proceedings—The 1987 Coalbed Methane Symposium, The University of Alabama, Tuscaloosa, Alabama, November 16-19: Gas Research Institute, The University of Alabama, and the U.S. Department of Labor, sponsors, p. 243-253.

Evans, K., Holzhausen, G., and Wood, M.D., 1982, The geometry of a large-scale nitrogen gas hydraulic fracture formed in Devonian shale: An example of fracture mapping with tiltmeters: Society of Petroleum Engineers Journal, v. 22, no. 5, p. 755-763.

Ljung, L., 1987, System identification: Theory for the user: Prentice-Hall Inc., Englewood Cliffs, N.J.

Mendenhall, W., 1975, Introduction to probability and statistics, 4th edition: Duxbury Press, Massachusetts, 460 p.

Nielsen, P.E., and Hanson, M.E., 1987, Analysis and implications of three fracture treatments in coal at the USX Rock Creek site near Birmingham, Alabama, *in* Proceedings—The 1987 Coalbed Methane Symposium, The University of Alabama, Tuscaloosa, Alabama, November 16-19: Gas Research Institute, The University of Alabama, and the U.S. Department of Labor, sponsors, p. 105-112.

Press, F., 1965, Displacements, strains and tilts at teleseismic distances: Journal of Geophysical Research, v. 70, no. 10, p. 2395-2412.

Press, W.H., Flannery, D.P., Teukolsky, S.A., and Vetterling, W.T., 1986, Numerical recipes: Cambridge University Press, Cambridge, England.

Schraufnagel, R.A., Lambert, S.W., Stubbs, P.B., Dobscha, F.X., and Boyer, C.M., II, 1987, The Rock Creek field laboratory—A project update, *in* Proceedings—The 1987 Coalbed Methane Symposium, The University of Alabama, Tuscaloosa, Alabama, November 16-19: Gas Research Institute, The University of Alabama, and the U.S. Department of Labor, sponsors, p. 83-91.

Smith, M.B., Ren, N.K., Sorrels, G.G., and Teufel, L.W., 1985, A comprehensive fracture diagnostics experiment, Part II, Comparison of seven fracture azimuth measurements: Society of Petroleum Engineers Paper 13894.

Smith, M.B., Ren, N.K. Sorrels, G.G., and Teufel, L.W., 1986, A comprehensive fracture diagnostics experiment, Part 2-Comparison of fracture azimuth measuring procedures: Society of Petroleum Engineers Production Engineering, v. 1, no. 6, p. 423-431.

Willis, R.M., Wright, T.B., Buharali, A.M., and Ely, J. W., 1987, Monitoring and analysis of coal-bed fracturing operations using the GRI mobile test and control facility, *in* Proceedings—The 1987 Coalbed Methane Symposium, The University of Alabama, Tuscaloosa, Alabama, November 16-19: Gas Research Institute, The University of Alabama, and the U.S. Department of Labor, sponsors, p. 319-323.

Wood, M.D., and Allen, R.V., 1973, Methods for prediction and evaluation of tidal tilt data from borehole and observatory sites near active faults: Philosophical Transactions of the Royal Society of London, v. 274, no. 1239, p. 33-36.

Wood, M.D., Parkin, C.W., Yotam, R., Hanson, M.E., Smith, M.B., Abbott, R.L., Cox, D., and O'Shea, P., 1983, Fracture proppant mapping by use of surface superconducting magnetometers: Society of Petroleum Engineers SPE/DOE paper 11612.